



BE CIVIL ENGINEERING PROJECT REPORT

EXPERIMENTAL ANALYSIS OF FLY ASH BASED GEOPOLYMER CONCRETE USING RECYCLED MATERIALS REPLACEMENT FOR USE AS COLUMN MATERIALS IN GROUND IMPROVEMENT

**Project submitted in partial fulfilment of the requirements for the
degree of BE CIVIL ENGINEERING**

PROJECT ADVISOR Dr ARSHAD ULLAH

SYNDICATE MEMBERS

(CMS 325126)	Capt Muhammad Hassan (Syndicate Leader)
(CMS 325110)	Capt Akram Hussain
(CMS 325105)	Capt Mubashir Mehmood
(CMS 325108)	Capt Usman Haroon

**MILITARY COLLEGE OF ENGINEERING NATIONAL UNIVERSITY
OF SCIENCES & TECHNOLOGY RISALPUR CAMPUS, PAKISTAN**

(2023)

This is to certify that the Final Year Design Project

**EXPERIMENTAL ANALYSIS OF FLY ASH BASED GEOPOLYMER
CONCRETE USING RECYCLED MATERIALS REPLACEMENT FOR**

SUSTAINABLE COLUMN MATERIALS AND GROUND IMPROVEMENT IN CONSTRUCTION

SUBMITTED BY

(CMS 325126) Capt Muhammad Hassan (Syndicate Leader)

(CMS 325110) Capt Akram Hussain

(CMS 325105) Capt Mubashir Mehmood

(CMS 325108) Capt Usman Haroon

Has been accepted towards the partial fulfilment of the requirement for **BE**
CIVIL ENGINEERING DEGREE

Dr Arshad Ullah

(Project Advisor)

Department of Transportation & Geotechnical Engineering

Military College of Engineering

National University of Science and Technology

DEDICATION

Dedicated to our parents, siblings, our instructors at MCE who have guided us during the course of this research and our great institution MCE where we have spent the four most memorable years.

DECLARATION

I certify that research work entitled “*an* experimental analysis of fly ash, slag and quarry rock dust based geopolymer concrete and its applicability as column materials and ground improvement in construction” is my own work. The work has not been presented elsewhere for assessment. Where material has been utilized from other sources it has been properly acknowledged/referred.

ACKNOWLEDGEMENTS

All praises to Almighty Allah Subhanhy WA Ta'Alla who gave us a chance to complete our work successfully. A Journey is easier when you travel together. This project is the result of extensive research and work whereby we have been accompanied and supported by many people. It is a pleasant aspect that we have now the opportunity to express our gratitude for all of them. We would also like to give our profound gratitude to our project advisor Dr Arshad Ullah whose guidance and expert opinions have provided us with the correct direction in undertaking all the tasks connected to the fulfilment of the project. Lastly, we would like to thank all the researchers out there whose publications we have consulted for the completion of this project.

ABSTRACT

The reuse of waste materials can help to solve problems relating to placing them in landfills and can be a step towards environmental sustainability by decreasing the production demand of cement for concrete. The use of Geopolymer concrete is one of the possible solutions that is rapidly gaining popularity among researchers. In this study, an attempt has been made to produce fly ash based geopolymer concrete using recycled waste materials replacement such as slag and quarry rock dust for construction. Four geopolymer concrete composites including normal concrete mixture, fly ash based geopolymer concrete containing 5% cement, fly ash and slag (1:1) based geopolymer concrete and fly ash, slag, and rock quarry dust (1:0.9:0.1) based geopolymer concrete were produced. Sodium hydroxide with molarity of 14 and sodium silicate solutions were used as an alkaline activator in this research.

The mechanical properties of the concrete composites were evaluated by conducting compressive strength test, tensile strength test and flexural strength test. It was found out that 50% fly ash, 45% slag & 5% quarry rock dust based geopolymer concrete cured at higher temperatures of 65 C showed an increase of 8% compressive strength at 28 days when compared with that of control mix of 28 days, whereas FGPC with 5% cement admixture showed an increase of 16% in 28 days compressive strength from the control mix. Similarly, the 28 days flexural strength of 50% fly ash, 45% slag & 5% quarry rock dust based geopolymer concrete was slightly higher than FGPC with 5% cement as an admixture and 4% down in flexural strength with that of control mix at 28 days. Cost analysis for all sample, which indicates that the sample composed of 5% Cement + GPC has the lowest cost among all the batches and almost 25% less than OPCC. Although all batches have the same size. Moreover, the 5% QRD + 45% Slag & 50% FA cost is 15 - 18% less than OPCC. After comparing all batches having different composition, it becomes evident that the 50% FA + 50% Slag is 10% cheaper than OPCC.

TABLE OF CONTENT

Title

Page

Dedication	III
Declaration	IV
Acknowledgements	V
Abstract	VI
List of Figures	X
List of Tables	XII
List of Abbreviations	XIV

CHAPTER	1:	INTRODUCTION
.....	1	
1.1		General
.....	1	
1.2	Fly Ash (Class F) Based	Concrete
.....	2	
1.3	Problem	Statement
.....	2	
1.4	Objectives	of Project
.....	2	
1.5	Scope	of Work
.....	3	
1.6	Sustainable Development Goals	(SDGs)
.....	3	
1.7	Project Report	Outline
.....	4	

CHAPTER	2:	LITERATURE	REVIEW
.....	5		
2.1	Effects of Concrete	on Environment	
.....	5		
2.2	Fly Ash		
.....	5		
2.3	Use of Fly Ash	in Concrete	
.....	7		
2.4		Geopolymers	
.....	7		
2.5	Source Materials	for Geopolymers	
.....	8		

2.6	Alkaline	Liquids	9
.....			
2.7	Overview of Fly Ash (FA) Modified	Concretes	9
.....			
2.7.1	Concrete Incorporating High Volumes of ASTM Class F Fly Ash		9
.....			
2.7.2	Durability characteristics of steel fiber reinforced geopolymer concrete		11
.....			
2.7.3	Influence of alkaline activators on the mechanical properties of fly ash based geopolymer concrete cured at ambient temperature		12
.....			
2.7.4	Development and Properties of Low Calcium Fly Ash Based Geopolymer Concrete		13
.....			
2.7.5	Feasibility study of ambient cured geopolymer concrete – A review		17
.....			
2.8	Conclusions form Literature Review		18
.....			
METHODOLOGY			20
.....			
3.1		Introduction	20
.....			
3.2	Materials used in this study		20
.....			
3.2.1	Fly Ash		20
.....			
3.2.2	Fine Aggregates		21
.....			
3.2.3	Coarse Aggregates		22
.....			
3.2.4	Alkaline Liquid		23
.....			
3.2.5	Super Plasticizer		24
.....			
3.3	Mixture Proportions		24
.....			
3.4	Manufacturing Process		25
.....			

3.4.1	Liquid	Preparation	25
3.4.2	Mixing of Materials and	Casting	26
3.4.3		Curing	27
3.5	Test	Matrix	28
3.5.1	Compressive	Strength Test	28
3.5.2	Splitting	Tensile Strength Test	29
3.5.3	Three Point	Loading Test	29
3.6		Summary	30
CHAPTER	4: RESULTS AND DISCUSSION		31
4.1		Introduction	31
4.2	Compressive	Strength Test	31
4.3	Splitting	Tensile Test	32
4.4	Three-Point	Loading Test	33
4.5	Numerical Modeling of Columns Supported Embankments		
4.5.1	Introduction		
4.5.2	Properties of materials		
4.5.3	Deformed mesh		
4.5.4	Numerical Modeling results		
4.5.4.1	Unreinforced model		
4.5.4.1.1	Stress settlement relationship		
4.5.4.1.2	Load carrying capacity at ground failure.		
4.5.4.1.3	Fly Ash & Slag based column reinforced models.		
4.5.4.2	Numerical Modeling		

4.5.4.2.1	Kaolin Clay					
4.5.4.2.2	Embankment					
4.5.4.2.3	Columns					
4.5.4.2.4	Rigid plate					
4.5.4.2.5	Plaxis 3D Modelling details					
4.5.4.2.6	Mesh formation					
4.5.4.2.7	Stage construction					
4.6	Cost	Benefit			Analysis	
.....						42
4.6.1	OPCC	Rigid	Pavement	Cost	Analysis	
.....						42
4.6.2	FGPC	Rigid	Pavement	Cost	Analysis	
.....						43
4.6.3	5% Cement + FGPC	Rigid	Pavement	Cost	Analysis	
.....						44
	4.6.4 Comparison Between Costs of Different Batches					
.....						45
4.7						Summary
.....						46
CHAPTER 5: CONCLUSION AND RECOMMENDATIONS						
47						
5.1						Introduction
.....						47
5.2	Manufacturing					Process
.....						47
5.3						Conclusions
.....						48
5.4						Recommendations
.....						48
References						
50						

LIST OF FIGURES

Figure Description	Page
Figure 2.1 Schematic Equation of Geopolymer Material	

.....	8	Figure 2.2 Effect of Curing Temperature on Compressive Strength	15
Figure 2.3 Effect of Curing Time on Compressive Strength			16
Figure 2.4 Effect of Super plasticiser on Slump of Concrete			16
Figure 2.5 Effect of Super plasticiser on Compressive Strength			17
Figure 3.1 Fly ash			21
Figure 3.2 Fine Aggregates			22
Figure 3.3 Coarse Aggregates			24
Figure 3.4 Chemicals for Preparation of Alkaline liquid			26
Figure 3.5 Preparation of Alkaline Liquids			27
Figure 3.6 Mixing of Concrete			27
Figure 3.7 Casting of Concrete			28
Figure 3.8 Dry Curing of FGPC in Oven			29
Figure 4.1 Comparison of Compressive Strength			33
Figure 4.2 Comparison of Splitting Tensile Strength			34
Figure 4.3 Three-Point Loading Test (Modulus of Rupture)			35
Figure 4.4 OPCC Design Parameters			38
Figure 4.5 OPCC Design Results			39
Figure 4.6 FGPC Design Parameters			39

Figure 4.7 FGPC Design Results 40

Figure 4.8 FGPC + 5% Cement Parameters..... 40

Figure 4.9 FGPC + 5% Cement Design Results..... 41

LIST OF TABLES

Table Description	Page
Table 2.1 Chemical Composition of Fly Ash as per ASTM C618-19	6
Table 2.2 Geopolymer applications offered by Davidovits based on the molar ratio of Si to Al.....	8
Table 2.3 Mechanical Properties of HVFA Hardened Concrete	10
Table 2.4 Effect of Molarity of NaOH and ratio Alkaline Solutions on Compressive Strength of FGPC	14
Table 3.1 Chemical Composition of Fly Ash	21
Table 3.2 Sieve Analysis of Fine Aggregate	22
Table 3.3 sieve Analysis of Coarse Aggregate	23
Table 3.4 Mixture Proportion of Control and Modified Batches	25
Table 3.5 Number of Specimens for Tests	29
Table 4.1 Compressive Strength Test Data	32
Table 4.2 Splitting Tensile Strength Data	33
Table 4.3 Three-Point Loading Test Data	34

Table 4.4 Thicknesses of Pavements for Various Batches

..... 37

Table 4.5 Stress and Deflection values for different batches

..... 38 Table 4.6 Comparison Between Values Calculated

Manually and by PAVExpress 41 Table 4.7 OPCC Cost / m³

..... 42 Table 4.8 OPCC

Total Cost 43 Table

4.9

FGPC Cost / m³ 43

Table 4.10 FGPC Total Cost

..... 44 Table 4.11 FGPC +

5% Cement Cost / m³ 44 Table 4.12

FGPC + 5% Cement Total Cost 45

Table 4.13 Comparison of Costs

..... 46

LIST OF ABBREVIATIONS

Abbreviations	Description
FA	Fly Ash
OPC	Ordinary Portland Cement
GPC	Geopolymer Concrete
F&SGPC	Fly ash & Slag based geopolymer concrete
FGPC	Fly Ash based Geopolymer Concrete
OPCC	Ordinary Portland Cement Concrete
ASTM	American Society for Testing and Materials
GGBS	Ground Granulated Blast Furnace Slag
ACI	American Concrete Institute
MCE	Military College of Engineering

CHAPTER 1

INTRODUCTION

1.1 General

Concrete is regarded as the most widely used material in the construction industry. Cement is a primary source that can be used as a binding agent in typical OPC concrete. Ordinary Portland cement concrete is associated with a number of environmental risks (OPCC). Burning Conventional hydrocarbons and calcining lime are required for OPC production, which results in significant amount of greenhouse gasses emissions such as carbon dioxide (CO₂) and NOX. According to current estimates, one tonne of CO₂ is generated in the production of one tonne of OPC (Kriven, et al, 2010). According to estimates that 1.6 billion tonnes of cement are manufactured each year, which results in generating CO₂ and adversely affecting the the environment and causes several health issues like asthma, bronchitis, and sinus infections (Cooper, et al, 2010.).

In contrast, more than 8000 coal power plants around the world produce billions of tonnes of fly ash (FA) from burning coal for energy generation. Some of the portion of the fly ash has been used in the concrete production, but still some of the fly ash is discarded in landfills. The utilization of fly and other recycled materials in concrete production are quietly desirable to reduce the threat to environment. Previous researchers used FA in OPCC in varying percentages as a partial replacement for OPC.

Fly ash reacts with calcium hydroxide to form (C-S-H) gel when used in place of some OPC in concrete in the presence of water. However, the partial replacement of cement is not enough to reduce the greenhouse gases, hence, another new material termed as geopolymer concrete is used.

In the 1980s, Joseph Davidovits made the first suggestion that "binders can be made via a polymeric reaction between alkaline liquids, silicon, and alumina in source materials such as FA and rice husk ash; he gave these binders the name geopolymers" (Davidovits, 1999). Alkaline liquids can be used to activate pozzolans

like FA to create a binder that can completely replace OPC in concrete. (Hossain, et al,2015)

This would occur as the pozzolan's calcium and silica react with the alkaline activator, creating C-S-H gel as the primary binder.

Researchers are also currently looking into the use of geopolymer concrete, which uses concrete as its primary building component, as column material and ground improvement. Researchers are considering using FGPC to address the issue since it uses less energy and emits less CO₂ than OPC-based concrete, which has been well established to emit large amounts of greenhouse gases that have a negative impact on the environment.

1.2 Problem Statement

The production of Concrete requires a significant amount of cement, which in turn results in release of greenhouse gasses in to the atmospheric One tonne of cement production release one tonne of CO₂ into the atmosphere. The construction industry need to find alternative sources of concrete production in order to counteract the high costs associated with relying on a single material (cement).Due to a variety of factors, including the price of fuel, the price of electricity, and the availability of raw materials, cement prices fluctuate significantly in the market. Nowadays researchers are focusing to utilize recycled materials for producing green concrete known as geopolymer concrete. Several researchers focused on utilizing fly ash as a silicate source in geopolymer concrete for various construction purposes. However, the use of blended recycled materials such fly ash, slag and quarry rock dust still need to be investigated in production of geopolymer concrete for use as a column material and ground improvement in construction..

1.3 Objectives of Project

As previously mentioned, extensive research has already been conducted on t his subject at the national and international levels, including analyses of the behavior of FGPC-cast beams and columns and their long-term effects on durability.

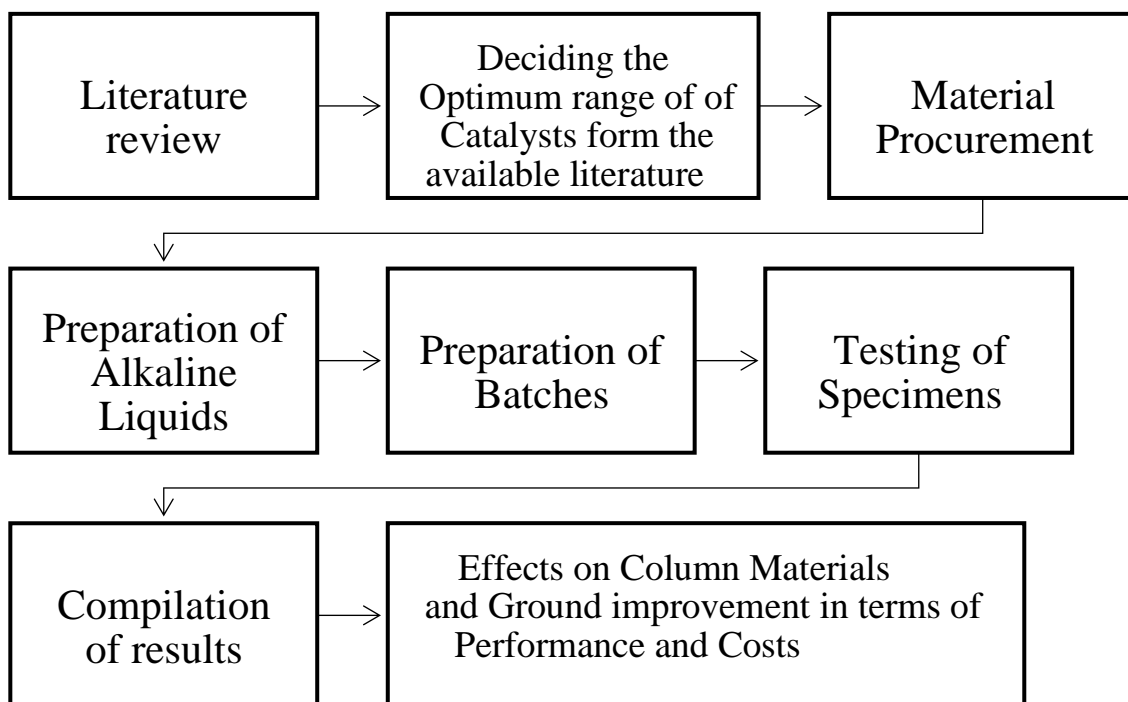
This project's primary goal was to compare four similarly designed specimens of a mix made of OPCC, FGPC with cement, F&SGPC, and FGPC with

QRD admixture under typical field conditions and environmental factors that exist in Pakistan.

The objectives envisioned for the projects were as follows:

- To evaluate the effectiveness of the FGPC for general use
- To examine the mechanical strength such as compressive strength, split tensile strength, and flexural strength of geopolymer concrete samples.
- To carry out a cost-benefit analysis of the use of FGPC in the construction of column materials & ground improvement.

1.4 Scope of Work



Fly ash, Slag and QRD was procured as a binder material for making FGPC. Alkaline liquids were procured from a chemical manufacturer in Rawalpindi. The same method of production and equipment was used for making FGPC as is used

for OPCC. It was envisaged that the characteristics of concrete were affected by their compressive, tensile, and flexural strengths.

1.5 Sustainable Development Goals

The following highlighted sustainable development goals which were adopted by the UNGA in 2015 are:

- GOAL 1: No Poverty
- GOAL 2: Zero Hunger
- GOAL 3: Good Health and Well-being
- GOAL 4: Quality Education
- GOAL 5: Gender Equality
- GOAL 6: Clean Water and Sanitation
- GOAL 7: Affordable and Clean Energy
- GOAL 8: Decent Work and Economic Growth
- **GOAL 9: Industry, Innovation and Infrastructure**
- GOAL 10: Reduced Inequality
- **GOAL 11: Sustainable Cities and Communities**
- **GOAL 12: Responsible Consumption and Production**
- **GOAL 13: Climate Action**
- GOAL 14: Life Below Water
- GOAL 15: Life on Land
- GOAL 16: Peace and Justice Strong Institutions
- GOAL 17: Partnerships to achieve the Goal

1.6 Project Report Outline

The project report is arranged in following manner:

Chapter 1: Introduction

Chapter 1 consists of the production of cement, energy consumed during manufacturing of cement, and estimation of CO₂ amount released during the production of cement in an open atmosphere and alternative of OPC to minimize the emission of CO₂, problem statement, and required objective of present research work.

Chapter 2: literature review

Chapter 2 contains a brief review of the literature on ground improvement, concrete, and geopolymer technology. Additionally, it explores the use of low-calcium fly ash concrete and the use of alternative binders to concrete (ASTM Class F).

Chapter 3: Research Methodology

Chapter 3 Describes the research strategy used to investigate the subject.

The procedure for carrying out various tests will be covered and explained in this chapter. This chapter will also explain the tests that are used to examine the behaviour of concrete.

Chapter 4: Tests and Results

Chapter 4 The test results are collected and discussed. On this page, we will talk about how the mechanical properties of concrete are affected using fly ash in concrete and curing conditions. The effects of FGPC use in rigid pavement are also explained in terms of the thicknesses attained for the various mix types taken into consideration in this study, and a cost-benefit analysis was also done.

Chapter 5: Conclusions and Recommendations

Chapter 5 will have the summary and conclusion part of the project report and few recommendations will also be given.

The project report will end with a reference list.

CHAPTER 2

LITERATURE REVIEW

2.1. Background of geopolymers

In 1978, the new family of minerals named geopolymers was introduced with an amorphous structure by Professor Joseph Davidovits as binders. This was the classification of solids resources, manufactured by the reaction of an alkaline liquid and an aluminosilicate powder. At that time, the initial purpose of the researchers on these new techniques (geopolymers) was to discover a new fire-resistant binding material because of the high extent of fires in Europe. The main concentration shifted to the usage of these binders in the construction industry, it was possible subsequently by the observation that to produce reliable and high-performance concrete with cementitious characteristics when fly ash was used with alkaline liquid (Provis et al. 2009).

2.2 Effects of Concrete on Environment

Buying and selling carbon permits and certificates is known as carbon trading. For many businesses, including the cement industry, carbon trading is a crucial control mechanism to keep track of the amount of greenhouse gas emissions that cause the rise in global temperature and climate change. To achieve sustainable goals for the benefit of the environment, these trading mechanisms are used to incentivize industry to cut their emissions. According to V. Malhotra (1999), "one tonne of carbon emission can have a trading value of about US \$ 10."

According to McCaffrey (2002), cement production is increasing by roughly 3% annually. "The production of one tonne of cement results in the release of approximately one tonne of carbon dioxide (CO₂) into the atmosphere." OPC production is responsible for 1.35 billion tonnes, or 7%, of the world's total greenhouse gas emissions (V. Malhotra, 2002). OPC is one of the most energy-intensive building materials, along with steel and aluminium.

The concrete industry has acknowledged these issues. For instance, "Vision 2030: "A Vision for the U.S. Concrete Industry". The statement states that "concrete technologists must guide future growth in a way that preserves environmental quality while pushing concrete as a preferred construction material. Concern from the public over climate change brought on by an increase in greenhouse gas concentrations will be carefully addressed. According to this perspective, concrete can continue to be a popular building material for

infrastructure projects while simultaneously being a more environmentally friendly material in the future (Mehta, 2001).

2.3 Fly Ash

Fly ash is described as "the finely divided residue that results from the combustion of ground or powdered coal and that is transported by flue gases from the combustion zone to the particle removal system" (ACI Committee, 2004) by the American Concrete Institute (ACI) Committee 116R. Fly ash is cleaned from the combustion gases using a dust collecting device that is positioned in the power plant's chimney before the gases are released into the atmosphere. Either manually or electrostatically is possible here. Fly ash fragments typically have a spherical shape with a diameter of between 1 micron and 150 microns, in contrast to OPC and lime.

The characteristics of the burning coal are used to categorise the chemical composition of FA. Fly ash, which is largely made up of silicon, aluminium, iron, and calcium oxides (CaO), also contains trace amounts of potassium, sodium, titanium, and sulphate. Bituminous coal and other types of coal with a higher iron content burn more effectively than coal with a lower calcium level. The kind of combustion, the kind of coal utilised, and the particle form all have an impact on physical and chemical properties (V. Malhotra & Ramezaniapour, 1994).

Class C fly ash, also known as high-calcium fly ash, is created when subbituminous coals are burned because it often contains more than 20% CaO in its ash. Fly ash that complies with ASTM Class F specifications and has a low calcium content is made from bituminous and anthracite coals. Fly ash's chemical make-up and material content determine its colour. in 1994 (V. Malhotra & Ramezaniapour). Table provides further information on both class F and class C. 2.1.

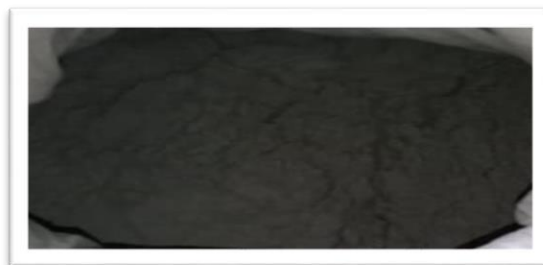


Fig 2.1: Fly Ash

Table 2.1 Chemical Composition of Fly Ash as per ASTM C618-19

Description	Class F	Class C
SiO₂ + Al₂O₃ + Fe₂O₃	50	50
CaO (%)	18 (max)	>18
SO₃ (max %)	5	5
Loss on Ignition (max %)	6.0	6.0
Moisture Content (max %)	3.0	3.0

Fly ash has following advantages over OPC as has been investigated by many researchers:

1. Inexpensive material
2. Better Mechanical properties
3. Suitable for high temperature curing conditions
4. Better durability and strength properties
5. Available as a by product of coal combustion

2.4 Quarry Rock Dust (QRD)

Quarry rock dust used in the production of geopolymer concrete in current research work was obtained from the bottom of stone crushers. The required size of QRD was obtained by grinding in the ball mill at PCSIR Peshawar. The main source of QRD is Margala hills. The process of QRD to obtain the required size and the chemical composition is shown in figure below and table 2.1 respectively.



Quarry rock dust used in the production of geopolymer concrete in current research work was obtained from the bottom of stone crushers. The required size of QRD was

obtained by grinding in the ball mill at PCSIR Peshawar. The main source of QRD is Margala hills. The process of QRD to obtain the required size and the chemical composition is shown in figure below and table 2.2 respectively.

Table 2.2: chemical properties of QRD

Chemical composition		
Compound	Test results	Units
SiO ₂	9.35	%
Al ₂ O ₃	1.64	%
Fe ₂ O ₃	1.03	%
CaO	47.13	%
MgO	1.25	%
K ₂ O	0.20	%
Na ₂ O	-0.11	%
SO ₃	0.08	%
Loss on Ignition	38.65	%
Moisture	0.80	%
Aluminum Ratio	1.59	-
Silica Ratio	3.51	-
L.S.F	1.64	-

2.5 Ground granulated blast furnace slag (GGBFS)

GGBFS is the waste product which is produced by slaking molten iron or steel slag from a blast kiln in steam or water. After that, the product appear granular and glassy is fully dried and then grounded into fine dust known as GGBFS. In the production of GPC, GGBFS has been utilized as a blended material to improve the fresh and harden properties of geopolymer binders with alumina-silicate sources (Li, Sun, and Li 2010). Currently used GGBFS is shown in figure below and Chemical composition and physical parameters are described in table 2.3.



Figure 2.3

Table 2.3: Chemical composition and physical parameters of GGBFS

Characteristic	Requirement as per ASTM: C989/Grade 80	Test results (%)
Chemical composition		
CaO	-	37.33
SiO ₂	-	34.38
Al ₂ O ₃	-	12.98
MgO	-	5.59
Fe ₂ O ₃	-	1.29
K ₂ O	-	0.82
Na ₂ O	-	0.29
SO ₃	4% max	0.23
Total alkalis	Min 0.66 max 0.90 %	0.85
Physical parameters		
Fineness by air permeability (cm ² /g)	-	4730

Amount retained when wet screened 45 μ (%)	Max 20 %	17.80
7 days	-	50
28 days	70 min	76

2.6 The demand for Geopolymer concrete

To produce eco-friendly concrete, we must use a new technique by replacing cement with some alternative binding materials which should not generate any bad effect on the environment. By using industrial by-products and some other waste materials having cementitious and pozzolanic properties as binders can reduce the environmental problems. In this admiration, a new technology geopolymer concrete is an encouraging technique. To reduce global warming, the geopolymer technology could diminish the emission of CO₂ to the atmosphere produced by aggregates and cement industries about 80% (Davidovits, 1994c). By using industrials and other wastes materials properly can reduce the problem of disposing and dumping waste products into the open atmosphere.

2.7 Geopolymer Nomenclature and Chemistry

To represent a wide range of the materials categorized by networks or chains of inorganic molecules, the geopolymer term was first invented by Davidovits in 1978. The mineral molecules in geopolymers are linked by chains or networks with a covalent bond. Geopolymer is prepared by the polymeric reaction of the alkaline solution with materials of geological origin source, by-products or waste materials such as GGBFS, fly ash, baggas ash, rice husk ash, etc. Because in this case of the polymerization process, a chemical reaction takes place. Davidovits invented the term 'Geopolymer' to characterize these binders. The chemical composition of geopolymers is like Zeolites but the amorphous structure can be formed. Geopolymers are chemically designated by the term proposed by Davidovits 'poly (sialate)' grounded on slico-aluminate. An abbreviation 'Sialate' is for silicon-oxo-aluminate.

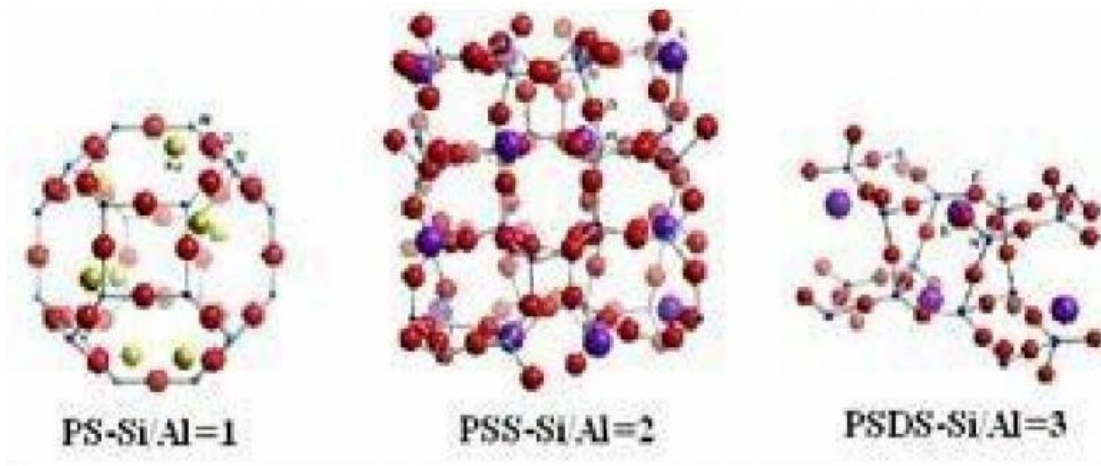


Figure 2.4

2.8 Alkaline Liquids

The most common alkaline liquid used in geopolymerization is likely a mixture of sodium hydroxide (NaOH) or potassium hydroxide (KOH) and sodium silicate or potassium silicate. (Barbosa, MacKenzie, & Thaumaturgo, 2000).

Palomo et al. (1999) determined that the type of alkaline liquid utilised in the polymerization reaction has a significant impact on the polymerization process. When sodium or potassium silicate is included in an alkaline solution, the reactions occur more quickly than when other alkaline hydroxides are used. Xu and Vans Deventer (2000) confirmed that combining sodium silicate solution with sodium hydroxide solution enhances the reaction among the parent material and the solution. Furthermore, it was discovered that the NaOH solution dissolved more material than the KOH solution, on average.

2.9 Concrete Incorporating High Volumes of ASTM Class F Fly Ash

Giaccio and Malhotra (1988), examined the mechanical characteristics of Types I and III cement-based high volume fly ash HVFA concrete. They created eight different concrete combinations, each 0.06 m³ in volume, with a w/c ratio of 0.32 using twelve batches of concrete. They kept the other ingredients the same while substituting fly ash for 60% of the cement in the mixture.

This investigation examined "12 x (152 by 305 mm cylinders), 192 x (102 by 203 mm cylinders), and 40 x (76 by 102 by 406 mm) prisms." Results from compression, flexion, splitting-tensile, and elasticity tests are displayed in Table 2.4.

Table 2.4 Mechanical Properties of HVFA Hardened Concrete, Giaccio and Malhotra (1988)

ASTM Type	Mixture No	Density at Day kg/m ³	Compressive Strengths of 102 by 203 mm Cylinders, MPa			28-day Flexural Strength of 76 by 102 by 406 mm Prisms, MPa	28-day Splitting Tensile Strength of 102 by 203 mm Prisms, MPa	28-day Modulus of Elasticity of 305 mm Cylinders, GPa
			1-d	7-d	28-d			
I	1 (Batch A)	2420	8.4	18.3	30.7	4.6	3	
	1 (Batch B)	2440			31.6			34.4
	2 (Batch A)	2400	9.3	17.6	32.5	4.9	3.3	
	2 (Batch B)	2420			33.3			35.5
	3 (Batch A)	2430	8.4	17.1	28.9	4.3	3.1	
	3 (Batch B)	2420			30.5			34
	4 (Batch A)	2410	9.6	17.5	29.2	5.2	3.2	
	4 (Batch B)	2420			31.9			35
III	5	2430	14.3	22.9	34.3	5.6	3.1	
	6	2425	13.8	24.0	34.8	5.6	3.2	
	7	2450	15.3	25.0	37.3	5.8	3.4	
	8	2435	14.8	26.3	37.7	6.2	3.6	

Concrete produced using Type I cement had a maximum one-day compressive strength of 9.6 MPa and a 28-day strength of 33.3 MPa respectively . Low C3S and C2S concentrations in Type I cement explains these inadequate strengths at one day. The compressive strengths of Type III cement after one day are much higher than

those of Type I cement concrete, with a maximum compressive strength 15.3 MPa which is about 37 % more than that of Type 1 cement.

The 28-day flexural strengths of the concrete produced with Type I cement and those of other similar-strength concrete produced with Type III cement are not significantly different from one another. Additionally, these values match those that experts for OPCC of a comparable strength have reported.

The highest 28-day splitting tensile strength of Type I cement was 3.3 MPa, whereas the maximum tensile strength of Type III cement was 3.6 MPa. The splitting tensile strength values are 10% of the 28-day crushing strength results, according to published statistics. These tensile strengths are comparable to those of a typical OPCC with an identical mix ratio.

A Young's modulus of elasticity of 35 GPa has been established using only Type I cement. A typical limestone concrete with the same strength has an elasticity modulus that is around 20% higher. E values are high because concrete particles have a densifying impact at 28 days, when there is little pozzolanic interaction between Portland cement and low-calcium fly ash.

Class F fly ash concrete has excellent mechanical properties, according to a study by Giaccio and Malhotra (1988), and it has great potential for structural concrete sections, especially large ones. For enough workability to be achieved in the early stages of construction, structural concrete with a significant proportion of fly ash appears to require the use of ASTM Type III cement and superplasticizers. According to this study, it

2.10 Workability

Various methods are in practice to find the workability of freshly made concrete and from those tests, the slump test is used to measure the workability (consistency) of fresh concrete. Measuring workability by this method is very simple and economical. It can be used anywhere either in the lab or in the field (site). This test should be accomplished precautionary despite its easy usage due to the reality that a minor distraction in the method will cause a large value of slump. The relief (ease) with which freshly prepared concrete can easily be provided any required shape by applying a load known as the workability (consistency) of concrete. The amount of disruption attained under some

circumstances depend on the viscosity of the grout or volume part (fraction) of the shear opposition (resistance) of the binding resources. Following the procedure given in ASTM C143-15a, the workability of concrete is measured by slump value and was achieved for each mix of OPC and GPC before casting (Fatihhi et al. 2019).

2.11 Compressive Strength

The maximum resistance proffered (faced) by the specimens of concrete either by cubes or cylinders during axial loading is known as compressive strength. The compressive strength is supreme common among all tests of hardened concrete, as it is performed easily without any disturbance and its many of the essential properties are qualitatively related to its compressive strength. The compressive of prepared OPC and GPC cylinder of each mix was subjected to a universal testing machine (UTM) and calculated through this test.

For determination of compressive strength of cylinder, the fresh concrete was poured in to steel moulds of well-oiled cylinder (150 mm x 300 mm). The steel cylinder were filled by fresh concrete in the three layers, and each coat (layer) of OPC mix was condensed with 25 blows by steel rod having dia of 25 mm and GPC mix was compacted by the electric vibrator to remove the pores and air in the cylinder. The demoulding of specimens was done after 24 hours of casting. Then OPC specimens were stored in the water tank and GPC specimens were placed in the oven at 65 °C for 48 hours. The testing of OPC specimens was done at the required age after taking out from water tank and GPC specimens was done at 7 and 28 Days receptivity. Reading the average value of three specimens was noted at the respective age.

2.12 Splitting tensile strength test

The tensile strength is a major and elementary property of concrete. Though, due to the brittle nature of concrete, it is not designed for direct tension resistance while applying load on concrete. The knowledge of tensile strength has considerable importance in calculating loads that can produce/develops cracks in the concrete specimens. The concrete specimens (cylinders) having dimensions of 150 mm dia and 300 mm height were used to find the tensile strength. OPC and GPC cylinders were placed under UTM in a horizontal plane at the age of 7 and 28 days for testing. ASTM C496/496M-04 (Vogel et al. 2008) was used to calculate the tensile strength of OPC and GPC samples. For

each 7 and 28 days, three OPC and GPC cylinders were tested, and average reading was noted and taken as split tensile strength (psi) and the following equation was used for the determination of tensile strength.

$$F_t = \frac{2P}{\pi DL} \quad (2.1)$$

Where,

F_t = Splitting tensile strength (Mpa),

P = Applied compressive load (N),

D = Diameter of cylinder (mm^2),

L = Length of cylinder (mm)

2.13 Flexural Strength

Third point loading test on the specimens of OPC and GPC to bending strength was performed to find the modulus of rupture (MOR) of prisms samples having dimensions of 100 mm x 100 mm x 500 mm. Following ASTM C78/C78M-16 (Shoaei et al. 2017), a flexural strength test was completed on the prisms samples. The MOR was noted by taking the mean value of three specimens. When the load was applied to the prism, the cracks and fracture were observed and noted within 2/3 part of the span length of the prism, which designated the formation of the tension surface in that region of the specimens. The three-point load test at the age of 28 days was carried for MOR of OPC and GPC samples of each group. The three-point loading test was carried under digital UTM in the laboratory. The following relation was used for the determination of MOR.

$$R = \frac{PL}{b d^2} \quad (2.2)$$

Where, R = MOR,

P = load (N),

L = specimen length

(mm), b = beam width

(mm), d = depth of beam

(mm)

2.14 Curing Temperature

After dry curing the test cylinders were kept in a furnace for 24 hours, while holding all other test variables constant, it was discovered that the compressive strength of both Mixtures 2 and 4 increased with increasing curing temperature. The compressive strength did not, however, appreciably rise as the curing temperature was raised over 60 C. Although it was shown that the FGPC reached its maximum strength at 90 C, most studies have chosen to cure the material at 60 C since up to this temperature, a rapid increase in compressive strength is seen. Figure 2.2 presents the data as a graph.

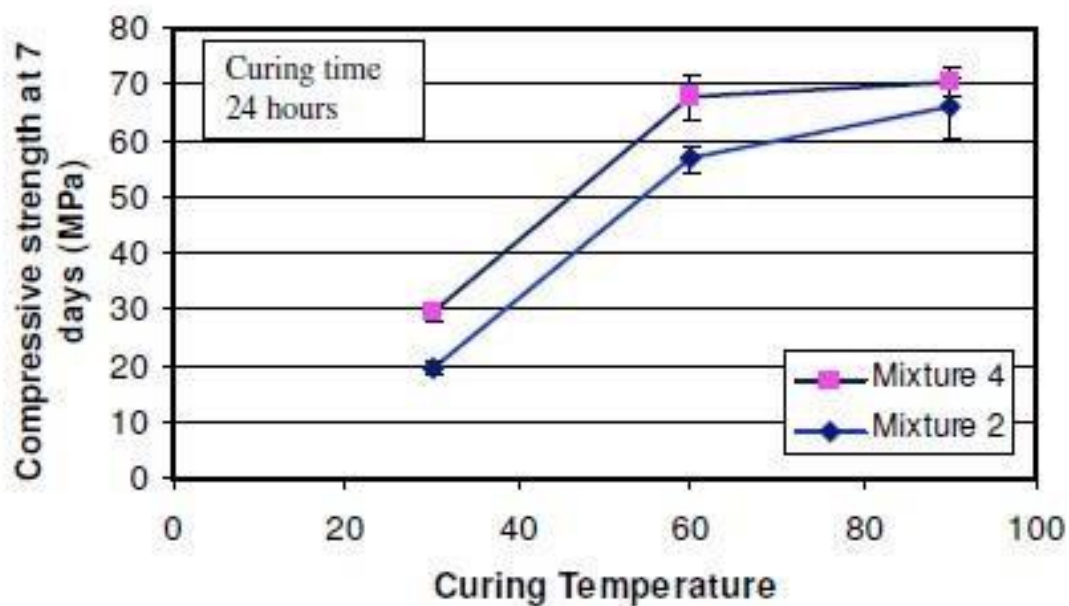


Figure 2.2 Effect of Curing Temperature on Compressive Strength (Hardjito & Rangan, 2005)

2.15 Effects of Curing Time on compressive strength of concrete

Longer curing durations were shown to enhance the polymerization process in concrete, which led to superior compressive strengths. The concrete quickly gained strength up to 24 hours after curing. After 24 hours, a considerable reduction in the rate of FGPC's strength development was seen. The enhanced polymerization

process of FGPC at higher temperatures and longer curing times is to blame for the increase in compressive strength over time. Figure 2.9 below depicts it in graphical form.

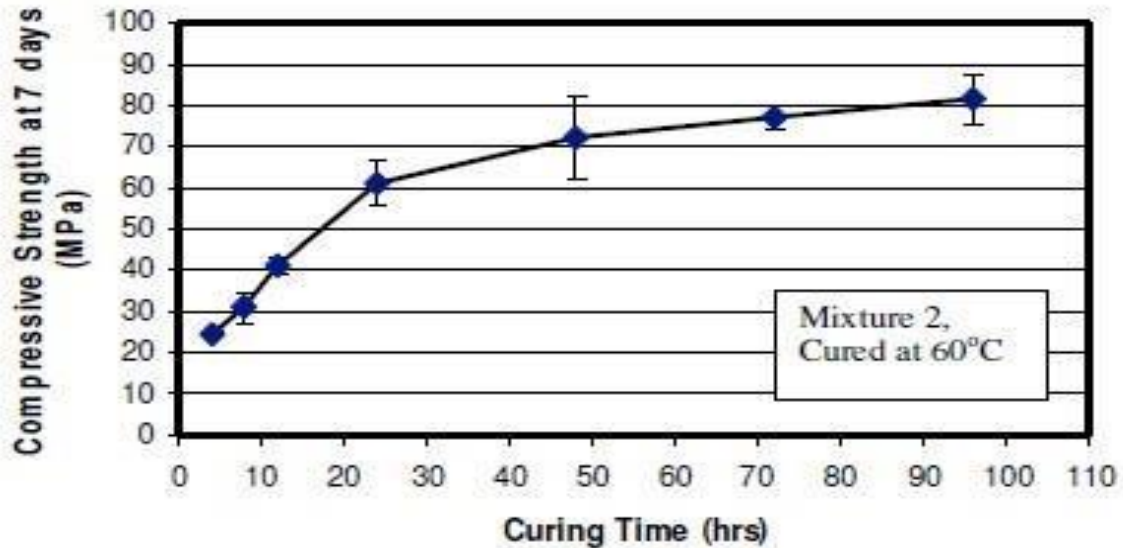


Figure 2.3 Effect of Curing Time on Compressive Strength (Hardjito & Rangan, 2005)

2.16 Conclusions form Literature Review

Certain characteristics relating to the manufacture and curing of FGPC were noticed after thorough review of the literature on the subject by various researchers.

For the purpose of this study, these parameters were established as guidelines for FGPC manufacture.

It was shown that the ideal concentration of NaOH for compressive strength in an alkaline solution is 14 M, with an average molarity of 8 M to 16 M. The best outcomes in terms of the mechanical properties of FGPC are obtained at a sodium silicate to sodium hydroxide ratio of 2.5. There are two ways to cure the FGPC: dry curing in an oven for 48 hours at an ideal temperature of 60 C or curing the FGPC at room temperature with the addition of an admixture. To help FGPC achieve the desired strength values at ambient curing temperatures, 5%–12% of cement is typically used.

CHAPTER 3

RESEARCH METHODOLOGY

3.1 Introduction

The experimental approaches used in accomplishing the objectives stated in chapter 1 are discussed in this section. Moreover, the approaches adopted in making the test specimens, details of used materials and different tests performing the procedure are discussed in this chapter. The sources of materials used, and their processing procedures are described in the detail. The different steps adopted in the production and, the testing of FA, GGBFS, and QRD based GPC.

There are several materials that can be utilised to make geopolymer concrete, but because fly ash (ASTM Class F) and QRD are readily available in Pakistan, we chose them for our project. The local market was used to purchase the cement. To ensure that the impacts of aggregate quality on fly ash and QRD characteristics were kept to a minimum.

3.2 Materials used in this study

3.2.1 Fly Ash

Fly Ash (FA) was procured for this project from the Rawalpindi. To create FGPC, it was employed as a complete replacement for cement (50% FA and 50% Slag). Since the fly ash utilised in that study was similarly collected from the same source, the chemical components of fly ash have been derived from (Abdullah, 2021). The fly ash was a light grey colour and had a texture like cement. According to its analysis, it had a CaO level of roughly 14.12%, indicating that it was the Class F fly ash that was needed for our investigation.

Table 3.1 Chemical Composition of Fly Ash (ASTM 2011)

SiO ₂ (%)	Al ₂ O ₃ (%)	Fe ₂ O ₃ (%)	CaO (%)	SO ₃ (%)	MgO (%)	LOI ^a (%)
59.96	14.02	6.29	14.12	2.84	0.41	0.445

$$(59.96+14.02+6.29=80.27 >50)$$

$$14.12 \leq 18$$

$$2.85 \leq 5$$

$$0.41 \leq 6$$

$$0.445 \leq 3$$

The results show that the amounts of SiO₂, Al₂O₃, and Fe₂O₃ were 80.27%, 14.12% for CaO, 2.85% for SO₃, and 0.445 for loss on ignition. This was class F fly ash because the proportion of CaO (14.12%), which is less than 18%, was so low.



Figure 3.1 Fly Ash

3.2.2 Fine Aggregates

We used the fine aggregates that were provided in the concrete laboratory for this study. These aggregates had a loose bulk density of roughly 1600 kg/m³. Below are the results of the fine aggregate's sieve analysis.



Figure 3.2 Fine Aggregates

Table 3.2 Sieve Analysis of Fine Aggregate

Sieve No.		Weight retained	% Retained	Cumulative % Retained	% Passing
No.	mm	(g)	(%)	(%)	(%)
#4	4.75	2	0.38	0.38	99.62
#8	2.36	3	0.60	0.98	99.02
#16	1.18	59	11	11.98	88.02
#30	0.6	132	24.9	36.88	63.15
#50	0.3	253	47.75	84.63	15.37
#100	0.15	56	10.60	95.23	4.77
#200	0.75	9	1.75	96.98	3.02
Pan	0	16	3	99.98	0

3.2.3 Coarse Aggregate

The concrete lab's coarse aggregate, which had an aggregate size range of 20 mm to 7 mm and a bulk density of 1794 kg/m³, was used in the same way as fine aggregate. The aggregate sample had an aggregate impact value of 22.73 percent and an aggregate crushing value of 22.55 percent. The sieve analysis for coarse aggregate is presented in Table 3.3

Table 3.3 Coarse Aggregate Sieve Analysis

Sieve No.	Weight retained	% Retained	Cumulative % Retained	% Passing
No.	(kg)	(%)	(%)	(%)
9.5	1	0.7	0.7	99.28
1/2	2.5	1.74	2.44	97.54
3/4	5	3.48	5.92	94.06

1	10	6.97	12.89	87.09
1^{1/2}	15	10.45	23.34	76.64
2	20	13.94	37.28	62.7
2^{1/2}	25	17.42	54.7	45.28
3	30	20.91	75.61	24.37
3^{1/2}	35	24.39	99.81	0.17
Pan	0.24	0.17	99.98	0



Figure 3.3 Coarse Aggregates

3.2.4 Quarry rock dust (QRD)

Quarry rock dust used in the production of geopolymer concrete in current research work was obtained from the bottom of stone crushers. The required size of QRD was obtained by grinding in the ball mill at PCSIR Peshawar. The main source of QRD is Margala hills. The process of QRD to obtain the required size and the chemical composition is shown in figure below and table 2.1 respectively.



Fig-Processing steps of Quarry rock waste

Table 2.1: chemical properties of QRD

Chemical composition		
Compound	Test results	Units
SiO ₂	9.35	%
Al ₂ O ₃	1.64	%
Fe ₂ O ₃	1.03	%
CaO	47.13	%
MgO	1.25	%
K ₂ O	0.20	%
Na ₂ O	-0.11	%
SO ₃	0.08	%
Loss on Ignition	38.65	%
Moisture	0.80	%
Aluminum Ratio	1.59	-
Silica Ratio	3.51	-

L.S.F	1.64	-
-------	------	---

2.2.5 Ground granulated blast furnace slag (GGBFS)

GGBFS is the waste product which is produced by slaking molten iron or steel slag from a blast kiln in steam or water. After that, the product appears granular and glassy is fully dried and then grounded into fine dust known as GGBFS. In the production of GPC, GGBFS has been utilized as a blended material to improve the fresh and harden properties of geopolymer binders with alumina-silicate sources (Li, Sun, and Li 2010). Currently used GGBFS is shown in figure below and Chemical composition and physical parameters are described in table 2.4.1.

Table 2.4.1: Chemical composition and physical parameters of GGBFS

Characteristic	Requirement as per ASTM: C989/Grade 80	Test results (%)
Chemical composition		
CaO	-	37.33
SiO ₂	-	34.38
Al ₂ O ₃	-	12.98
MgO	-	5.59
Fe ₂ O ₃	-	1.29
K ₂ O	-	0.82
Na ₂ O	-	0.29
SO ₃	4% max	0.23
Total alkalis	Min 0.66 max 0.90 %	0.85
Physical parameters		

Fineness by air permeability (cm ² /g)	-	4730
Amount retained when wet screened 45 μ (%)	Max 20 %	17.80
7 days	-	50
28 days	70 min	76

3.2.6 Alkaline Liquid

The main source of the alkaline liquids used to create GPC was a solution of sodium silicate (Na₂SiO₃) and sodium hydroxide (NaOH). Because they were less expensive and easily accessible on the local market.

By letting NaOH pellets dissolve in water, NaOH solution was made. The Molarity (M) of NaOH particles in water is used to calculate their mass. NaOH has a molecular weight of 40 g/L, hence a solution with a 14 M concentration of the molecule has a concentration of 560 g/L. When determining the mass of the solution, it is important to remember that water, not NaOH solids, make up the majority of the NaOH solution.

3.3 Mixture Proportions

To evaluate all other mixes against, a control mixture of OPCC was first created. The GPC mixture proportion that was previously reported was obtained from a previous study by Hardjito & Rangan (2005). It was decided to choose a mixture percentage that was similar to the control mixture proportion which is **1:1.5:3**. Below is the mixture proportions.

Table 3.4 Mixture Proportion of Control and Modified Batches

Materials	OPCC (kg/m ³)	FGPC + 5% 50% FA,		50% FA, 45% Slag,
		Cement (kg/m ³)	50% Slag (kg/m ³)	5% QRD (kg/m ³) +
Cement	403	20.4	-	-
Fly ash	-	387.6	102	102
Slag	-	-	225	202
QRD	-	-	-	65
Coarse Aggregate	1512	1512	1512	1512
Fine Aggregate	672	672	672	672
Sodium Silicate (SiO ₂ / Na ₂ O=2)	-	103	103	103
Sodium Hydroxide Solution	-	41	41	41
Water	241.8	22.5	22.5	22.5

3.4 Manufacturing Process

Standard operating procedures were followed to produce the control batch for the comparison's objectives because the OPCC manufacturing process is well-known. With a few exceptions, the FGPC manufacturing process is relatively similar to the OPCC one. The following manufacturing processes are used to produce FGPC:

- Preparation of liquids
- Mixing of materials and casting
- Curing of test specimens
- Conduct of testings

3.4.1 Liquid Preparation

Make the alkaline liquid first and then mix and pour the fly ash concrete a day later. The process of dissolving sodium hydroxide pellets in water is exothermic, which means that a lot of heat is produced as a result of the reaction. As a result, the sodium

hydroxide solution and sodium silicate solution were combined one day prior to the preparation of the mix's solid components.

The molarity 14 was chosen, determined the mass of sodium hydroxide pellets that were utilised to prepare the solution. The sodium hydroxide solution was created by dissolving 560 grams of NaOH per litre of water.

After making the sodium hydroxide solution, sodium silicate, the necessary amount of water was added. This mixing technique was adapted from prior studies (Wallah & Rangan, 2006). The solution was allowed to cool down over night in the lab in accordance with the literature because the mixing operation produced a tremendous amount of heat.



Figure 3.4 Chemicals for Preparation of Alkaline Liquid



Figure 3.5 Preparation of Alkaline Liquids

3.4.2 Mixing of Materials and Casting

In a concrete drum mixer, the mixture's solid components were combined for 2– 3 minutes before the liquid component was added, and the constituents were then blended for 5 minutes.

Three layers of mixed concrete were then manually poured and tamped with a rod for 25 blows into the 150 mm x 300 mm cylinders. By placing the cylinder on a vibrating platform for 10 seconds, each layer was likewise stabilised. The 100 mm x 100 mm x 100 mm prisms were similarly cast in two layers and stabilised by being placed on a vibrating table for 10 seconds after each layer had been tamped for 25 blows.

3.4.3 Curing

It is significant to remember that, FGPC does not require water for its curing process. To speed up the geopolymerization process inside FGPC and provide it the needed strength, dry or heat curing is required (Jindal, 2018).

To investigate their effects on the characteristics of GPC, two forms of curing were used. Dry oven curing was the first kind. The specimens were kept in their moulds for a day at room temperature after being cast. The specimens were removed from their moulds after a day and put in an oven in the Geotech lab at MCE. After being heated to 60°C in the oven for 48 hours, the specimen was once more exposed to ambient curing for 7 days.

The second method of curing was ambient curing, which involved adding 5% cement to the slurry as an additive to hasten the geopolymerization of the concrete while it was ambient curing at room temperature. The specimen was placed in its mould for this form of curing for 24 hours, after which it was removed and placed in a location in the lab where it would receive enough sunshine throughout the day to cure until the time of the application of the tests on that specimen.



Figure 3.8 Dry Curing of FGPC in Oven

3.5 Test Matrix

Table 3.5 Number of Specimens for Tests

Tests	Specimens			Age (days)	Type
	OPCC	50% FA, 50% Slag	50% FA, 45% Slag, 5% QRD		
Compressive Strength	3	3	3	7	Cylinders
	3	3	3	28	
Splitting Tensile Strength	3	3	3	7	Cylinders
	3	3	3	28	
Three Point Loading	3	3	3	7	Prisms
	3	3	3	28	

3.5.1 Compressive Strength Test

The structural dynamics lab, MCE, has a 3000 KN automatic servo plus machine that was used to evaluate the compressive strength of the specimens. The tests were carried out in compliance with [ASTM C39](#). Cylinders were 150 mm x 300 mm in dimension. The cylinders in the OPCC batch were taken out of the curing tank on days 7 and 28 and tested right away since, as per ASTM standard, the test must be conducted on moist specimens. Only on the seventh day were the FGPC specimens, which were dry-cured, obtained for testing. The FGPC specimen was examined for 7 and 28 days of strengths while it was oven cured for first 48 hours and the wrapped up in plastic sheets. The experiments were carried out at ambient room temperature. Due to the FGPC specimens' rough top and bottom surfaces, sulphur capping was performed on them. After applying sulphur to the cylinders' faces, the

specimens were allowed to cure for five hours before being tested. The appropriate testing mode was chosen from the machine's menu after the specimens had been loaded. The load was delivered at a stress-controlled rate of "0.25 MPa/s as per ASTM C39" during the test. When the specimen's ultimate strength was reached, the machine automatically stopped applying load. The machine interface was then used to note the compressive strength test findings.

3.5.2 Splitting Tensile Test

On the same (3000 KN automatic servo plus) machine that was used for compressive strength tests, the splitting tensile tests of the specimens were conducted. ASTM 496 was followed while performing the testing. Cylinders were 150 mm x 300 mm in dimension. The cylinders in the OPCC batch were taken out of the curing tank on days 7 and 28 and tested right away since, per ASTM standard, the test must be conducted on moist specimens. Only on the seventh day were the FGPC specimens, which were oven-cured, obtained for testing. The FGPC specimen was examined for 7 and 28 days of strengths. The experiments were carried out at ambient room temperature. The specimens were set in the steel jig to ensure that the bearing surface was correctly aligned. The appropriate test mode was then chosen for the testing mode once the jig had been installed in the machine. The test was a stresscontrolled test in which a load was delivered at a rate of "0.7 - 1.4 MPa/min as per ASTM 496". When the cylinder's maximum tensile strength was reached, the machine automatically stopped applying the load. The outcomes were then recorded in the machine's user interface

3.5.3 Three Point Loading Test

Prisms were used in the specimen loading tests for three points loading test. The tests were carried out in compliance with ASTM C293. Prisms have dimensions of 100 mm by 100 mm by 500 mm. The cylinders in the OPCC batch were taken out of the curing tank on days 7 and 28 and tested right away since, per ASTM standard, the test must be conducted on moist specimens. Only on the seventh day were the FGPC specimens, which were dry-cured, obtained for testing. The strength of the FGPC specimen under ambient curing conditions was examined after 7 and 28 days. The experiments were carried out at ambient room temperature. After attaching the

supporting blocks to the apparatus, which would serve as the prism's supports, the prism was set on the supporting blocks. In accordance with ASTM standards, a 25 mm gap was left between the point support and end face of the prism. The load-applying block was then placed on the centre point of the upper face of the prism. Without making any abrupt changes, the load was delivered to the specimen at a rate of 1 MPa/s, which was well within the ASTM standard range

3.6 Summary

This chapter went into great length on the FGPC preparation techniques, and the materials needed to produce FGPC concrete. It was discovered that the same manufacturing procedure utilised for OPCC may also be used to create GPC. Also mentioned was the control batch's mixture proportion and the modified batches. The research's tests will reveal information about the mechanical properties of concrete.

CHAPTER 4

RESULTS AND DISCUSSIONS

4.1 Introduction

This chapter portrayed the influence and effects of QRD with FA and GGBFS as a binder on GPC properties. The tests that were run during this investigation are related to the mechanical properties of the concrete. The test results from the subsequent tests are discussed here:

- Compressive Strength Test
- Splitting Tensile Test
- Three Point Loading Test

The impacts of all the batches of concrete used in this research will be studied after the data presentation. The information gathered during the testing was used to compute the thickness for a standard length of stiff pavement. A cost-benefit analysis was conducted for each type of batch used to determine the respective thicknesses after the thicknesses had been determined.

4.2 Compressive Strength Test

Table 4.1 Compressive Strength Test Data
Compressive Strength (psi)

Sample	7 Days	28 Days	Remarks
OPC (Control)	2993.58	3673.81	Water Cured
FGPC + 5% Cement	2849.99	3807.24	Oven Cured at 60° for 48 hours
50% FA, 50% Slag	2503.35	3512.8	“
50% FA, 45% Slag, 5% QRD	3002.28	3931.98	“

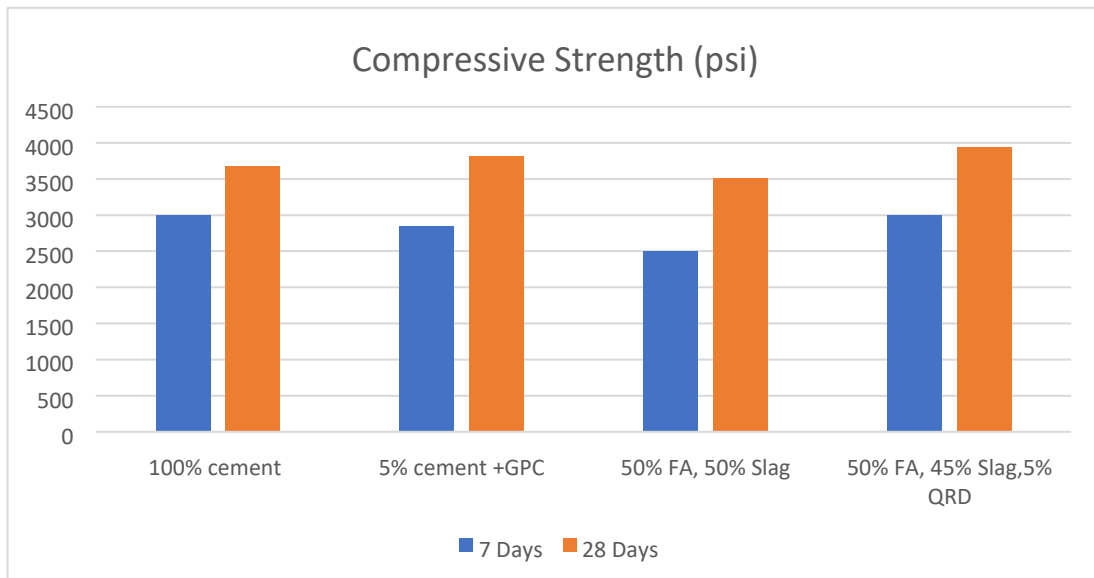


Figure 4.1 Comparison of Compressive Strength at 7 & 28 days of all Batches

Figure 4.1 makes it clear that out of all the batches, **50% FA, 45% Slag, 5% QRD** achieved the maximum 28-day compressive strength (2931.98 psi), around 7% higher than control and 3% more than sample 5% cement + FGPC and 11 % more than sample **50% FA, 50% Slag**

. The 28-day compressive strength of the concrete made with 5% cement and FGPC is the second highest (3807.24 psi), and it was roughly 4% higher than that of the control. The results clearly show that GPC batches were able to achieve compressive strengths that were higher than OPCC.

4.3 Splitting Tensile Test

Table 4.2 Splitting Tensile Test Data

Splitting Tensile (psi)			
Sample	7 Days	28 Days	Remarks
OPC (Control)	227.70	301.67	Water Cured
	169.69	200.15	
FGPC + 5% Cement			Oven Cured at 65° for 24 hours
50% FA, 50% Slag	210.30	253.81	“
50% FA, 45% Slag, 5% QRD	216.10	263.96	“

Table 4.2 Splitting Tensile Strength Data

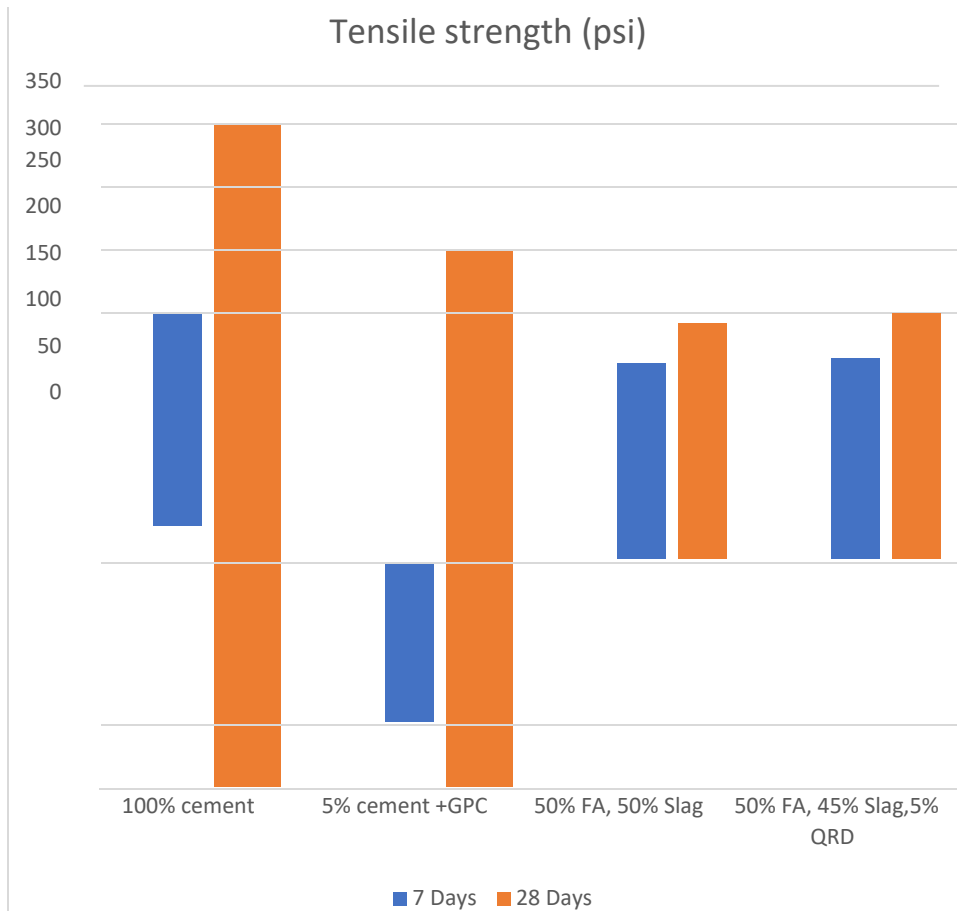


Figure 4.2 Comparison of Splitting Tensile Strength at 7 & 28 days of all Batches

Figure 4.2 makes it clear that 50% FA, 45% Slag, 5% QRD achieved the maximum 28day tensile strength (263.96 psi), around 13 % lower than control mix and 24% more than sample 5% cement + FGPC and 4 % more 50% FA, 50% Slag. The results clearly show that among all the batches of GPC, 50% FA, 45% Slag, 5% QRD had the highest tensile strength (263.96), followed by of 50% FA, 50% (263.96).

4.4 Three Point Loading Test

Table 4.3 Three-Point Loading Test Data
Three Point Loading Test (Modulus of rapture) (psi)

Sample	28 Days	Remarks
OPC (Control)	374.19	Water Cured
FGPC + 5% Cement	361.14	Oven Cured at 60° for 24 hours
50% FA, 50% Slag	355.34	“

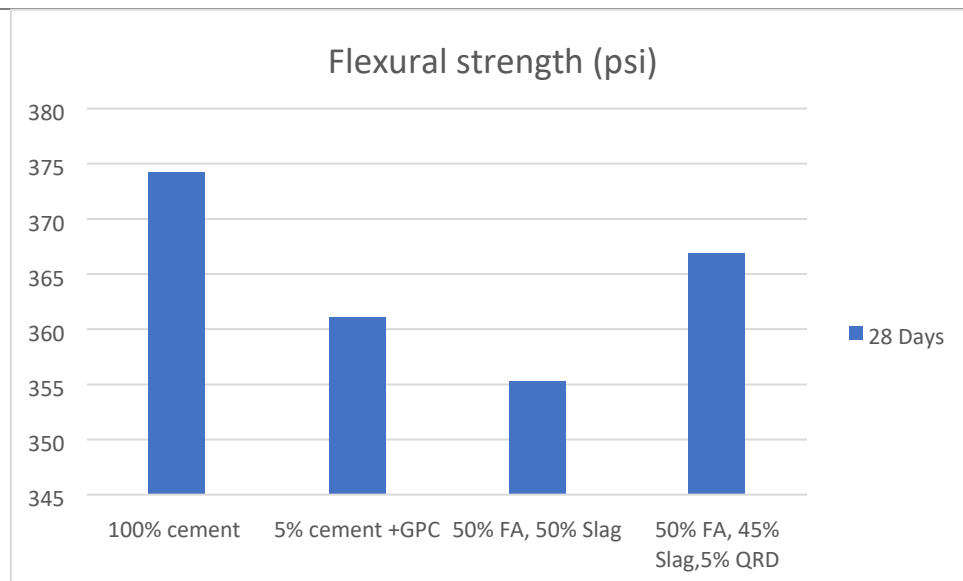


Figure 4.3 Three-Point Loading Test (Modulus of Rupture) at 7 & 28 days of all Batches

Figure 4.3 makes it clear that 50% FA, 45% Slag, 5% QRD achieved the maximum 28day flexural strength (266.94 psi), around 2% lower than control mix and 24% higher than sample 5% cement + FGPC and 4 % higher 50% FA, 50% Slag. The results clearly show that among all the batches of GPC, 50% FA, 45% Slag, 5% QRD had the highest flexural strength (266.94), followed by 5% cement + FGPC (261.14).

4.5 NUMERICAL MODELLING OF COLUMNS SUPPORTED EMBANKMENT

4.5.1 Introduction

The outcomes of the numerical simulations conducted using the Plaxis-3D Foundation's (finite element technique) software, which was licenced from University Technology Malaysia, are discussed in this chapter. The numerical modelling offers a thorough estimation of complex issues, enabling information to be obtained that is not feasible by other techniques. The stress settlement behaviour obtained from the laboratory loading tests was modelled using numerical analysis. In order to evaluate the load-carrying capacity under the same requirement—which specified the failure point as when the

settling of 10% of the footing width is achieved—a laboratory physical model was simulated in Plaxis 3D. Three area replacement ratios of 10.90%, 16.36%, and 21.83% were used in the numerical modelling, along with three-column lengths of 100, 150, and 200 mm ($L/D = 4, 6, \text{ and } 8$ correspondingly). In contrast to "P" for physical modelling, the code "N" will be utilised as the initial alphabet for the numerical analysis. However, to distinguish between the floating column lengths of 100 mm and 150 m, the L/D ratio has been included to the numerical modelling notation. For instance, P-PP-BC4-11 denotes a physical modelling test with partially penetrated bottom ash columns that have an area improvement ratio of 10.90% and a length to diameter ratio of 4. A parametric analysis was used to assess the performance of bottom ash, cement bottom ash, and geopolymer columns. Therefore, this chapter includes three portions, the numerical simulation results are discussed in the first portion, while the results of physical and numerical modelling were compared in the second portion and the third portion is related to the preliminary design charts.

4.5.2 Properties of Materials

The choice of material properties in numerical modelling is crucial for accurate simulations. To gather the soil parameters for the numerical modelling, laboratory tests were conducted, and some of the values came from earlier research. Consolidation and the vane shear test were used to attain the soft soil (clay) characteristics. Because the bottom ash was gathered from the same power station and has a nearly identical density, the modulus of elasticity for the bottom ash was used in the same manner as Moradi (2016). While the gradient of stress-strain relationship obtained from the unconfined compressive strength test was used to determine the modulus of elasticity for the cement bottom ash column and the geopolymer column. The cement bottom ash and geopolymer columns' respective moduli of elasticity were found to be 30 MPa and 50 MPa. While both cement bottom ash and geopolymer columns employed a Poisson ratio of 0.15. Using the linear elastic model, Chai et al. (2015) and Chai et al. (2017) simulated soil-cement columns and assigned the Poisson ratio of 0.15. Different parameters utilised in numerical modelling of foundation soil and columns, respectively, are shown in Tables 4.4 and 4.5.

Table 4.4 Parameters for numerical modelling of kaolin clay, embankment and rigid footing

Parameter	Kaolin clay	Embankment	Rigid footing
-----------	-------------	------------	---------------

Material model	Soft soil model	Embankment	
Drainage type	Undrained A	Undrained B	Nonporous
γ_d (kN/m ³)	16	15	24
γ_{sat} (kN/m ³)	18	18	
E (kN/m ²)	-	7500	2.4E7
ν	0.15	0.45	0.2
c	8	35	
C_c	0.29	-	
C_s	0.068	-	
Friction angle	16	-	
Permeability (m/sec)	2.227E-13		

Table 4.5 Parameters for different columns

Parameter	Bottom ash columns	Cement bottom ash columns	Geopolymer columns
Material model	Embedded beam	Linear elastic	Linear elastic
γ_d (kN/m ³)	10.76	20	22
E (MPa)	14	30	50
ν	0.3	0.15	0.15

4.5.3 Deformed Mesh

Figure 4.1 displays the deformed mesh produced for the unreinforced soil under embankment loading. Under the laden embankment piece, settling is more pronounced,

as may be observed. The ground heaves upward close to the embankment's toe. The embankment at the toe often moves as a result of the deformation under the loaded area pushing the foundation soil. The overall displacement of the embankment over soft soil due to surcharge loading is shown in Figure 6.2. It is obvious that there has been considerable displacement below the laden area and that it has extended to the embankment's toe. The numerical model's failure pattern and the laboratory model test had good agreement.

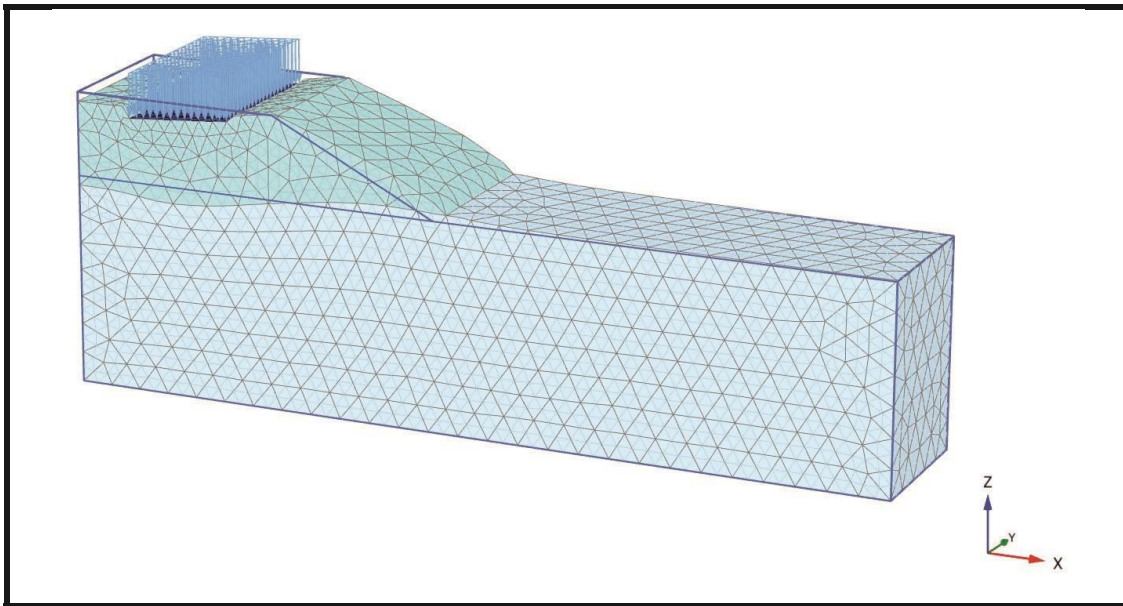


Figure 4.1 Deformed mesh of embankment with surcharge loading on soft soil

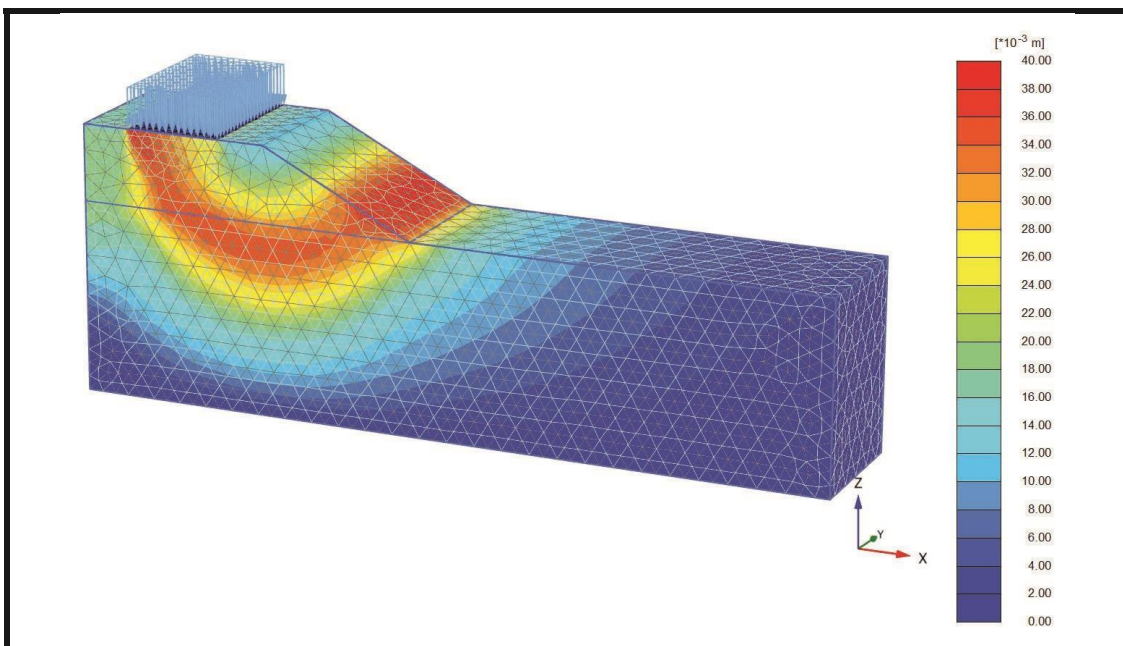


Figure 4.2 Total displacement of embankment on soft soil

4.5.4 Numerical Modelling Results

The results achieved from the numerical modelling for the unreinforced case, bottom ash columns, cement bottom ash columns and geopolymer columns reinforced clay under embankment loading are addressed in this section.

4.5.4.1 Unreinforced Model

In this section, the stress-settlement relationship and load carrying capacity for the unreinforced model is discussed.

4.5.4.1.1 Stress-Settlement Relationship

According to the numerical simulation, Figure 6.3 shows the relationship between stress and settlement for the unreinforced model. It is clear that the vertical tension rises continuously as settlement rises until it reaches a plateau at roughly 10mm settlement. When the vertical tension is raised further, the embankment's tendency to settle on unreinforced clay grows swiftly. The ground without reinforcement showed ductile behaviour, it was discovered.

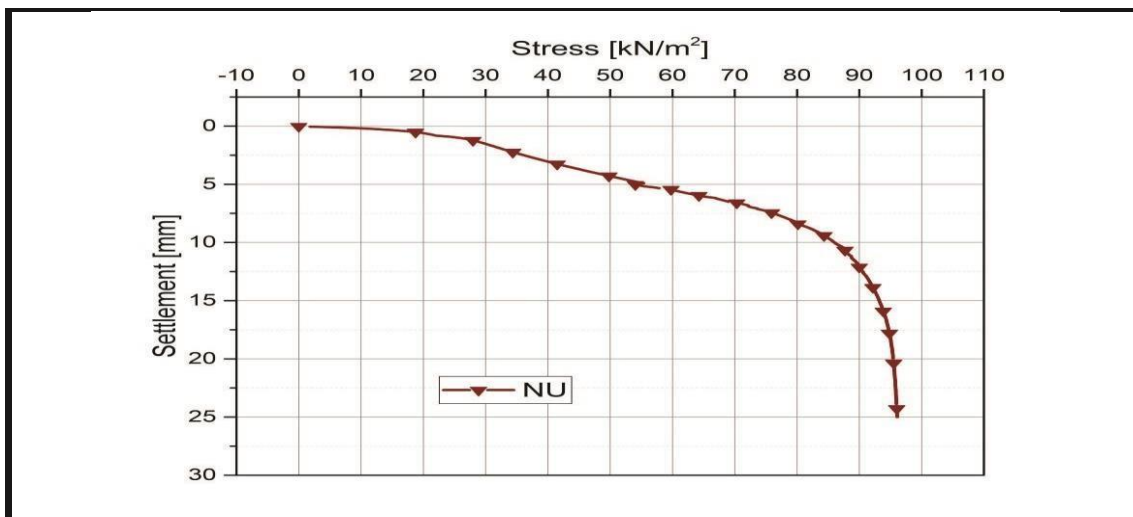


Figure 4.6 Stress-settlement relationship of the unreinforced clay subjected to the embankment with surcharge loading (Numerical Modelling)

4.5.4.1.2 Load Carrying Capacity at Ground Failure

The failure point was established by Terzaghi (1947) and Fattah et al. (2016a) technique when settlement reached 10% of the footing width, or 10 mm in this investigation. The embankment supported on unreinforced clay was found to have an ultimate load bearing capacity of 86 kPa. The load-bearing ratio was calculated using the clay's undrained shear strength to load-bearing capacity ratio. The achieved bearing ratio is 10.11, which corresponds to a settlement of 10% of the footing width.

4.5.4.1.3 Fly Ash & Slag based Columns Reinforced Models

In this section, the stress-settlement relationship, load-carrying capacity and improvement factor for the bottom ash columns reinforced models are discussed. **Table 4.7** Reinforced Models Details

Details	Test	Test label	c_u	Remarks
	11	P-FP-CC-22	9	Physical modelling test with fully penetrated cement bottom ash columns having a 21.81% area improvement ratio
Geopolymer columns	12	P-PP-GC-16	8.5	Physical modelling test with partially penetrated bottom ash based geopolymer columns having a 16.36% area improvement ratio
	13	P-FP-GC-16	8.5	Physical modelling test with fully penetrated bottom ash based geopolymer columns having a 16.36% area improvement ratio

4.5.4.2 Numerical Modelling

The stress-settlement behaviour of laboratory-scale physical modelling was the main subject of this study. Using the finite element method (FEM)-based computer

programme Plaxis 3D foundation version 2019, numerical simulations were used to confirm and support the results of physical modelling testing. To calculate and evaluate the stress-settlement behaviour of physical modelling and Plaxis 3D simulations, numerical analysis was done. The examination of challenges with interactive engineering makes good use of the finite element method. The software is a 3D finite element database created for the study of the foundation framework, according to the Plaxis 3D foundation manual. By adhering to graphical input parameters, this programme allows users to create interactive models. With the right material models, the interaction between the piles or columns supporting the embankment and the surrounding soil can be properly represented.

The column supported embankment on soft ground was simulated using a 3D model created in the Plaxis software. 15 triangular node elements were used in fine meshing to create the mesh for the object. Due to the larger stress concentration in the area of reinforced ground and embankment, the mesh was refined. Different soil models were used to simulate the behaviour of the embankment, soil, and columns. These models are addressed in the following sections.

4.5.4.2.1 Kaolin Clay

Given different conditions, soil exhibits a wide range of responses because of its highly nonlinear and time-dependent behaviour. To mimic the mechanical behaviour of soil, a variety of precisions are needed (Brinkgreve, 2005). As a result, when using numerical modelling to mimic soil behaviours, selecting the right model is crucial. The choice of the appropriate constitutive model to describe the behaviour of the soil in accordance with the specified demands is significantly influenced by the type of soil model, structure, and condition of loading.

The kaolin clay, which is typically used to represent the primary consolidation of soft soil, was chosen for the soft soil model (SSM). The SSM is a Cam-Clay type model that can replicate the compression behaviour of extremely soft soils because it was created for primary compression (Plaxis, 2019). Previous research (Chai et al., 2017; Chai et al., 2019) used a soft soil model to simulate the behaviour of soft clay under the embankment. The

Mohr-Coulomb failure criterion is followed by the SSM model's failure pattern. Modified compression index (O), modified swelling index (N), effective cohesion (c'), friction angle (l), and dilatancy angle () are the parameters needed for the SSM model.

The modified indices can be found through Equation. (3.3) and (3.4).

$$O = \frac{c_c}{2.3(1e)} \quad (4.1)$$

$$N = \frac{2c_s}{2.3(1e)} \quad (4.2)$$

In which e, c_c and c_s are the void ratio, compression index and swelling index. The SSM has an alternative option of c_c , c_s and e_{int} , which can be used to Automatically calculate the values of O and N .

4.5.4.2.2 Embankment

The Mohr-Coulomb model (MCM) undrained B was used to model the embankment in Plaxis 3D. For undrained soil layers with known undrained shear strength characteristics, MCM model with drainage type undrained B is employed. By setting the internal friction angle to zero and the cohesion to the undrained shear strength, this model directly takes the parameters of the undrained shear strength into account (Plaxis, 2013). The Poisson's ratio (Q), effective cohesion (c'), friction angle (l), and dilatancy angle () were the five input quantities needed by the MCM model. Chai et al. (2017) verified their design process by simulating two centrifuge models created by Inagaki et al. and employed a Poisson ratio of 0.45 for the embankment sitting on the deep mixed columns. (2002) and Kitazume and Maruyama (2006). The embankment was generated using create surface option and then extruded in the y-direction.

4.5.4.2.3 Columns

Two alternative modelling techniques, such as the embedded pile and isolated columns by volume approach employing the Mohr-Coulomb model, were used to represent the columns. The parameters relating the elastic modulus, unit weight, and column diameter are necessary for the embedded piles. The embedded pile can be placed anywhere in the foundation soil and connected to the surrounding soil by means of two special interfaces called tip and skin friction. An embedded beam element was used to represent the bottom ash columns. According to Figure 3.36, Moradi (2016) modelled the bottom ash column using an embedded pile element. The volumetric approach was utilised to generate the cement bottom ash and geopolymer columns, and a linear elastic model was applied to determine the material characteristics. The parameter required for the linear elastic material was unit weight, elasticity and Poisson ratio. Said (2019) modelled soil-cement columns by volume method as shown in Figure 3.37.

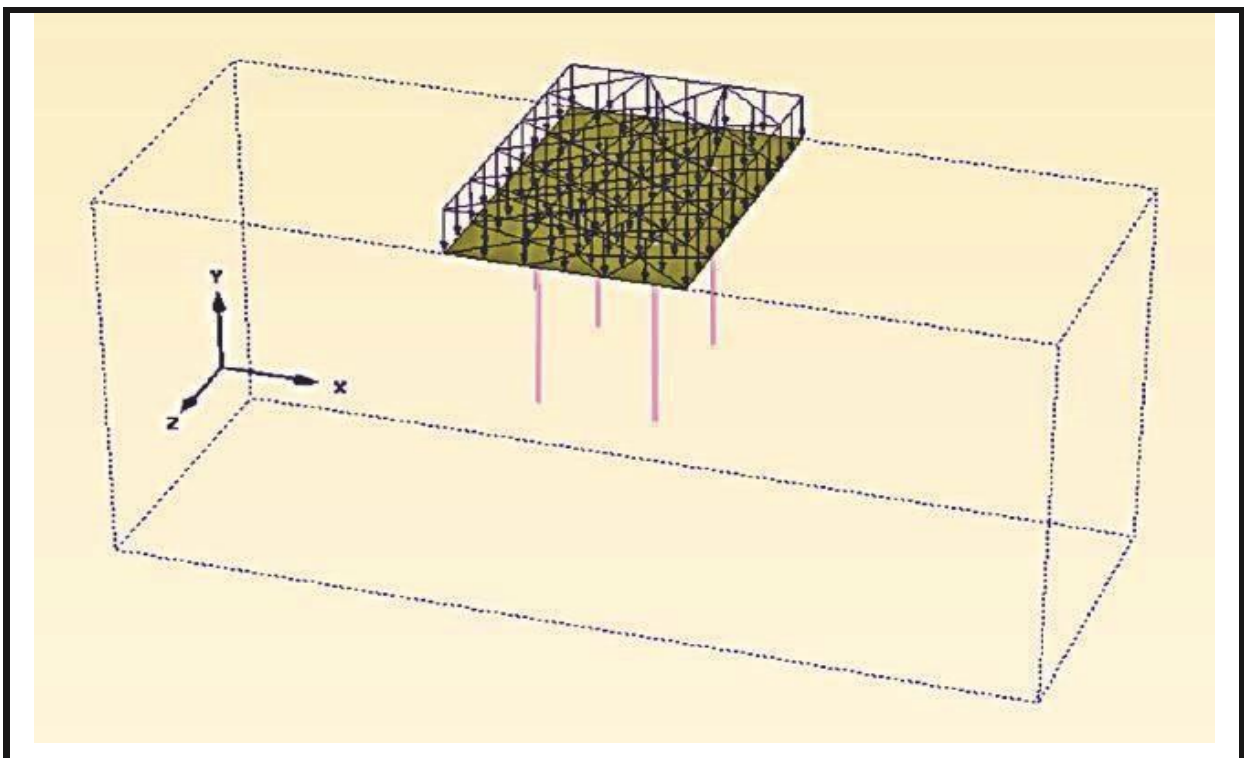


Figure 4.8 Numerical modelling of clay reinforced with four partially penetrated columns (Moradi, 2016)

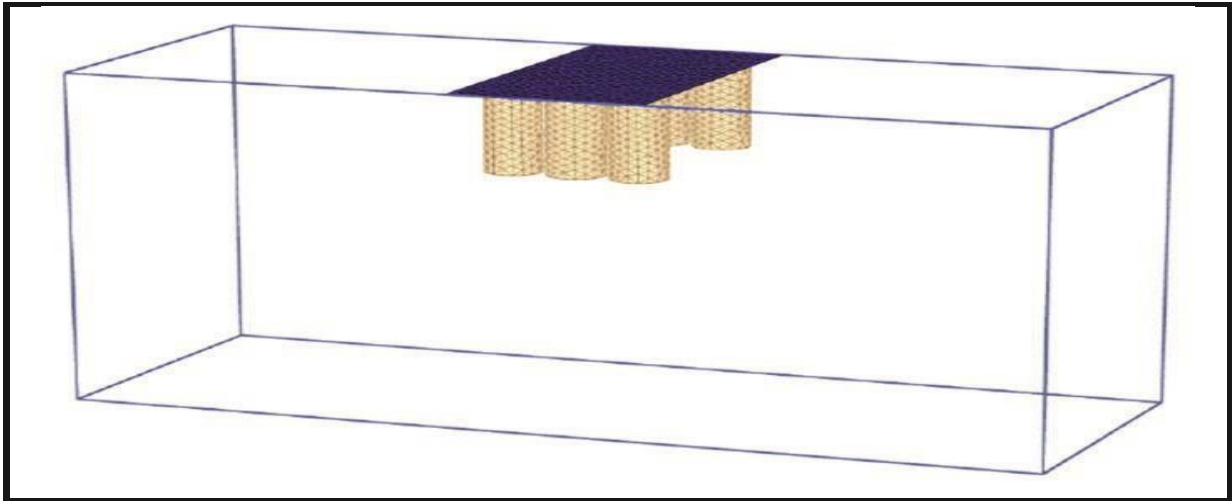


Figure 4.9 Numerical simulation of clay reinforced by six partially penetrated columns (Said, 2019)

4.5.4.2.4 Rigid Plate

The rectangular aluminum plate was placed on the embankment to distribute the load on the embankment surface homogeneously. In Plaxis 3D the footing was simulated as a plate by assigning the parameters unit weight, thickness of plate and elasticity modulus.

4.5.4.2.5 Plaxis 3D Modelling Details

By entering the dimensions' values, a soil geometry must be generated in order to analyse a 3D project. Through the use of a drill, the layer of kaolin clay's depth was determined. In the structure stage, models of the embankment and cement columns or embedded beams were created. Then, the relevant geometry element was given the properties of each material. The characteristics of various materials that had to be used in numerical modelling are described in Table 3.6. These stand for Soft soil model (SSM), Mohr-Coulomb model (MCM), embedded beam (EB), and linear elastic model (LEM), respectively. The materials' parametric values are reported in Figure 4.10 and 4.11

Figure 4.10 Input parameters for numerical simulations

Parameters	Kaolin Clay	Embankment	Bottom ash columns	Cement columns	Geopolymer columns	Rigid plate
------------	----------------	------------	--------------------------	-------------------	-----------------------	----------------

Material model	SSM	MCM	EB	LEM	LEM	
γ	✓	✓	✓	✓	✓	✓
E	✓	✓	✓	✓	✓	✓
ν	✓	✓	✓	✓	✓	✓
c'	✓	✓				
C_c	✓					
C_s	✓					
ϕ'	✓					

4.5.4.2.6 Mesh Formation

The mesh for the ground model was created when the model parameters were assigned. For the model, a fine mesh with 15 triangular node elements was used to create the global mesh. Due to the larger stress concentration in the area of reinforced ground and embankment, the mesh was refined. The mesh created for the reinforced clay model is shown in Figure 3.38.

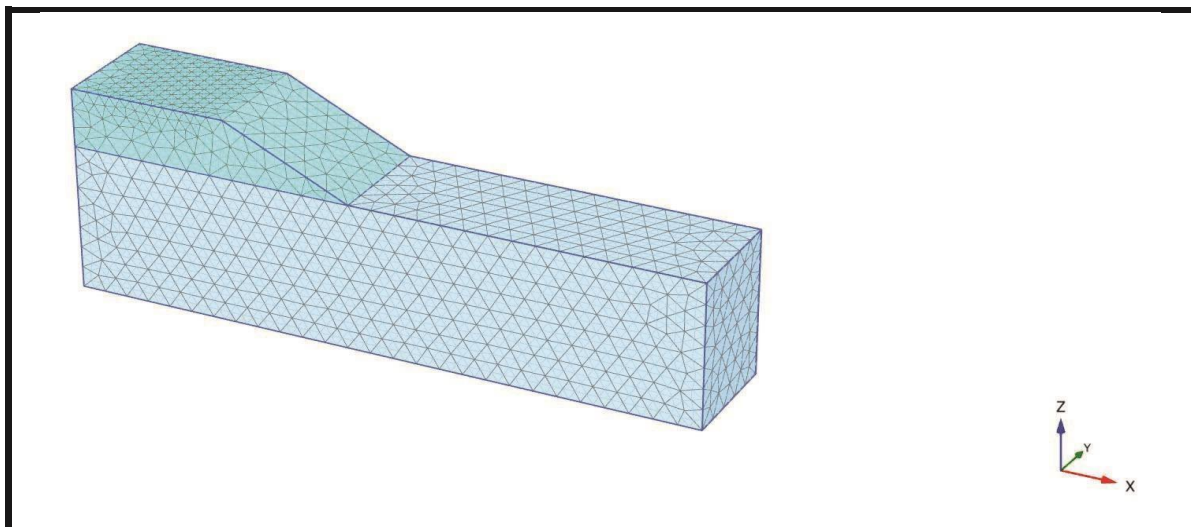
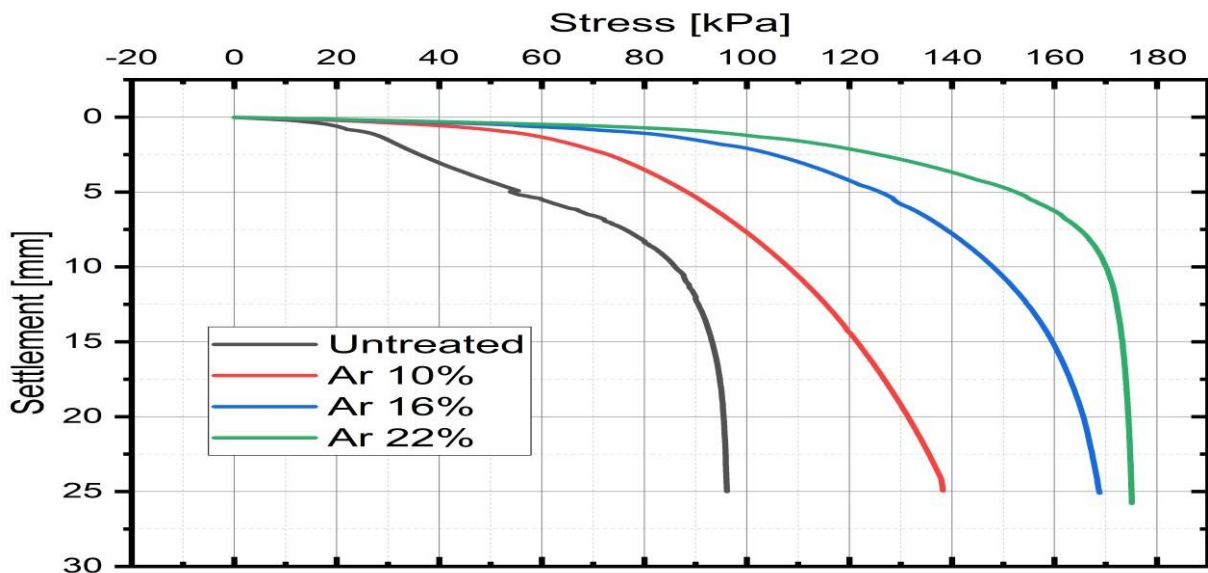


Figure 3.38 Mesh generated for the unreinforced clay model

4.5.4.2.7 Stage Construction

Three stages of stage construction were developed based on the stages of physical model testing. On the basis of the effective stress elements, the over consolidation ratio, and the pre-overburden pressure, the major stress history can be ascertained using the initial phase, which is also referred to as gravity loading or the K0 process. The lateral earth pressure coefficient at the initial stress stage is smaller in typically consolidated soil than in over consolidated soil. To determine the initial stresses, the clay layer was activated in the first step. The second phase involved the activation of an embankment on clay to ascertain the stresses created by the embankment's weight in the clay. The surface load was turned on to work on the embankment's top during the third phase.



4.6 Cost Analysis

The table below presents a comparison of the sample cost, which indicates that the sample composed of 5% Cement + GPC has the lowest cost among all the batches and almost 25% less than OPCC. Although all batches have the same size. Moreover, the data shows that the 5% QRD + 45% Slag & 50% FA cost 15 - 18% less than OPCC. After comparing all batches having different composition, it becomes evident that the 50% FA + 50% Slag is 10% cheaper than OPCC. The chemicals used in this process can only be obtained at a given cost when procured in bulk quantities. The significant

cost reduction between FGPC and OPCC mixtures indicates that a huge amount of capital can be saved on large-scale construction projects.

Table 4.7 OPCC Cost per cubic meter.

Constituents	Quantity (Kg/m³)	Cost Per Unit (Rs)	Total Cost (Rs/m³)
Cement	1440	30 / kg	43200
Coarse aggregate	1794	130 / ft ³	1089
Fine aggregate	1600	190 / ft ³	800
Total			Rs 18873

Table 4.8 FGPC Cost per cubic meter

Constituents	Quantity	Cost Per Unit (Rs)	Total Cost (Rs)
Fly Ash	240 Kg	7/ Kg	1680
Coarse aggregate	8.37 ft ³	130 / ft ³	1089
Fine aggregate	4.17 ft ³	190 / ft ³	800
Slag	240	20/ Kg	4800
QRD	1.83 ft ³	350	650
Na₂SiO₃	24.125 Kg	50 / Kg	2206
NaOH	11.65 kg	65 / Kg	1147
Total			Rs 7572

CHAPTER 5

CONCLUSIONS AND RECOMMENDATIONS

5.1 Conclusions

Based on the results obtained by testing of OPC and GPC mixes, the following conclusions were drawn:

- The low slump values of the workability of GPC mixes were observed due to the sticky nature of geopolymer concrete.
- The optimum slump value of 85 mm was observed for OPC concrete mixes. The workability of GPC mixes decreases due to the finess and flaky nature of GGBFS and QRD particles.
- Oven cured 50% FA, 45% Slag,5% QRD has greater 28-days compressive strength from OPCC (28-days) by up to 8%, this means that 50% FA, 45% Slag,5% QRD will have better application in areas where rapid construction under constrained time environment is required.
- OPCC highest tensile strength from all the batches; 5% cement +GPC (33%), 50% FA,50% Slag (16%) and 50% FA, 45% Slag,5% QRD (13%)
- In GPC, Oven cured 50% FA, 45% Slag, 5% QRD achieved the maximum 28day flexural strength (266.94 psi), around 2% lower than control mix and 24% higher than 5% cement + FGPC and 4 % higher 50% FA, 50% Slag
- From cost analysis it was found that sample composed of 5% Cement + GPC has the lowest cost among all the batches and almost 25% less than OPCC. Although all batches have the same size. Moreover, the data shows that the 5% QRD + 45% Slag & 50% FA cost 15 - 18% less than OPCC. After comparing all batches having different composition, it becomes evident that the 50% FA + 50% Slag is 10% cheaper than OPCC.

5.2 Recommendations

After the conduct of research following recommendation were proposed:

- Further research needs to be carried to find the short- and long-term effects of water curing on FGPC.
- The strength of the bond between FGPC and steel reinforcement, as well as their behaviors, require more investigation.
- To promote the usage of FGPC, it is necessary to cut the price of alkaline liquids like sodium hydroxide and sodium silicate and for that it is necessary to encourage their production at industrial scale by the local chemical industry.
- Further research is necessary to find out the application of geopolymer technology in other fields of construction.
- The fibers i.e., steel and polypropylene fibers can be used to enhance the mechanical properties of GPC based on FA, QRD, and GGBFS
- Fire tests on FA-QRD-GGBFS based GPC beams, slabs, columns, and other basic structural elements can be performed for better awareness of fire durability of GPC structural members.
- After exposure to high temperatures, the shear behavior of FA-QRD-GGBFS based GPC beams can be explored.
- Different cooling techniques can be used for alkali-activated FA-QRD-GGBFS based concrete specimens after exposure to elevated temperature.

References

- Ahmed, Gamal N, and James P Hurst. 1995. "Modeling the Thermal Behavior of Concrete Slabs Subjected to the ASTM E119 Standard Fire Condition." *Journal of Fire Protection Engineering* 7 (4): 125–32.
- Aliabdo, Ali A, Abd Elmoaty M Abd Elmoaty, and Hazem A Salem. 2016. "Effect of Water Addition, Plasticizer and Alkaline Solution Constitution on Fly Ash Based Geopolymer Concrete Performance." *Construction and Building Materials* 121: 694–703.
- Aslani, Farhad. 2016. "Thermal Performance Modeling of Geopolymer Concrete." *Journal of Materials in Civil Engineering* 28 (1): 4015062.
- Awal, A S M Abdul, and I A Shehu. 2015. "Performance Evaluation of Concrete Containing High Volume Palm Oil Fuel Ash Exposed to Elevated Temperature." *Construction and Building Materials* 76: 214–20.
- Buchanan, Andrew H, and Anthony Kwabena Abu. 2017. *Structural Design for Fire Safety*. John Wiley & Sons.
- Choate, William T. 2003. "Energy and Emission Reduction Opportunities for the Cement Industry." In *Energy and Emission Reduction Opportunities for the Cement Industry*. BCS, Incorporated.
- Davidovits, J. 1982. "The Need to Create a New Technical Language for the Transfer of Basic Scientific Information."
- Abdullah, M. (2021). *Investigating of Shear Behavior in Steel Reinforced Geopolymer Concrete Beams*. (Master of Science In Structural Engineering), University Of Engineering and Technology (UET), Lahore, Lahore.
- ACICommittee. (2004). Use of Fly Ash in Concrete. *American Concrete Institute*, 41.
- Barbosa, V. F., MacKenzie, K. J., & Thaumaturgo, C. (2000). Synthesis and characterisation of materials based on inorganic polymers of alumina and silica: sodium polysialate polymers. *International journal of inorganic materials*, 2(4), 309317.
- Cheng, T.-W., & Chiu, J. (2003). Fire-resistant geopolymer produced by granulated blast furnace slag. *Minerals engineering*, 16(3), 205-210.

- Davidovits, J. (1999). *Chemistry of geopolymeric systems, terminology*. Paper presented at the Geopolymer.
- Davidovits, J. (2002). Personal Communication on the Process of Making of Geopolymer Concrete.
- Deasai, J. (2004). Construction and performance of high-volume fly ash concrete roads in India. *Special Publication*, 221, 589-604.
- Ganesan, N., Abraham, R., & Raj, S. D. (2015). Durability characteristics of steel fibre reinforced geopolymer concrete. *Construction and Building Materials*, 93, 471476.
- Ghafoor, M. T., Khan, Q. S., Qazi, A. U., Sheikh, M. N., & Hadi, M. (2020). Influence of alkaline activators on the mechanical properties of fly ash based geopolymer concrete cured at ambient temperature. *Construction and Building Materials*, 273, 121752.
- Giaccio, G. M., & Malhotra, V. (1988). Concrete incorporating high volumes of ASTM Class F fly ash. *Cement, concrete and aggregates*, 10(2), 88-95.
- Gourley, J. (2003). *Geopolymers; opportunities for environmentally friendly construction materials*. Paper presented at the Materials 2003 Conference: Adaptive Materials for a Modern Society, Sydney, Institute of Materials Engineering Australia.
- Hardjito, D. (2005). *Studies of fly ash-based geopolymer concrete*. Curtin University.
- Hardjito, D., & Rangan, B. V. (2005). *Development and properties of lowcalcium fly ash-based geopolymer concrete*. Curtin University.
- Haseeb, J. (2017). Environmental Impact of Ordinary Portland Cement. Retrieved from <https://www.aboutcivil.org/environmental-impact-opc>
- Jindal, B. B. (2018). *Feasibility study of ambient cured geopolymer concrete—A review*. (6). (4)
- Jindal, B. B., Singhal, D., Sharma, S., Yadav, A., Shekhar, S., & Anand, A. (2017). Strength and permeation properties of alccofine activated low calcium fly ash geopolymer concrete. *Comput. Concrete*, 20(6), 683-688.
- Lloyd, N., & Rangan, V. (2010). *Geopolymer concrete with fly ash*. UWM Center for By-Products Utilization.

- Malhotra, V. (1999). Making concrete "greener" with fly ash. *Concrete international*, 21(5), 61-66.
- Malhotra, V., & Ramezani-pour, A. (1994). Effects of fly ash on durability of concrete. *CANMET, Natural Resources Canada, Ottawa, Ontario, Canada*.
- Malhotra, V. M., & Mehta, P. K. (2002). High-performance, high-volume fly ash concrete: materials, mixture proportioning, properties, construction practice, and case histories.
- Mehta, K. P. (2001). Reducing the environmental impact of concrete. *Concrete international*, 23(10), 61-66.
- Nath, P., & Sarker, P. K. (2015). Use of OPC to improve setting and early strength properties of low calcium fly ash geopolymer concrete cured at room temperature. *Cement and concrete composites*, 55, 205-214.
- Palomo, A., Grutzeck, M., & Blanco, M. (1999). Alkali-activated fly ashes: A cement for the future. *Cement and concrete research*, 29(8), 1323-1329.
- Sharma, C., & Jindal, B. B. (2015). Effect of variation of fly ash on the compressive strength of fly ash based geopolymer concrete. *IOSR J. Mech. Civ. Eng*, 42-44.
- Tahir, M. F. M., Abdullah, M. M. A. B., Hasan, M. R. M., & Zailani, W. W. A. (2019). *Optimization of fly ash based geopolymer mix design for rigid pavement application*. Paper presented at the AIP Conference Proceedings.
- Teixeira-Pinto, A., Fernandes, P., & Jalali, S. (2002). *Geopolymer manufacture and application-Main problems when using concrete technology*. Paper presented at the Geopolymers 2002 International Conference, Melbourne, Australia, Siloxo Pty. Ltd.
- Van Jaarsveld, J., Van Deventer, J., & Lorenzen, L. (1997). The potential use of geopolymeric materials to immobilise toxic metals: Part I. Theory and applications. *Minerals engineering*, 10(7), 659-669.
- Wallah, S., & Rangan, B. V. (2006). Low-calcium fly ash-based geopolymer concrete: long-term properties. 18.
- Xu, H., & Vans Deventer, J. (2000). The geopolymerisation of alumino-silicate minerals. *International journal of mineral processing*, 59(3), 247-266.

- Xu, H., & Vans Deventer, J. S. (2002). Geopolymerisation of multiple minerals. *Minerals engineering*, 15(12), 1131-1139.